MARTIN MARIETTA ENERGY SYSTEMS LIBRARIES
3 4456 0361461 2

CENTRAL RESEARCH LIBRARY
DOCUMENT COLLECTION

ORNL-2831
Controlled Thermonuclear Processes

CRITICAL CURRENT FOR BURNOUT IN AN OGRA-TYPE DEVICE

Albert Simon

CENTRAL RESEARCH LIBRARY
DOCUMENT COLLECTION
LIBRARY LOAN COPY
DO NOT TRANSFER TO ANOTHER PERSON
If you wish someone else to see this document, send in name with document and the library will arrange a loan.

OAK RIDGE NATIONAL LABORATORY
operated by
UNION CARBIDE CORPORATION
for the
U.S. ATOMIC ENERGY COMMISSION

Printed in USA. Price $1.50. Available from the

Office of Technical Services
Department of Commerce
Washington 25, D.C.

LEGAL NOTICE

This report was prepared as an account of Government sponsored work. Neither the United States, nor the Commission, nor any person acting on behalf of the Commission:

A. Makes any warranty or representation, expressed or implied, with respect to the accuracy, completeness, or usefulness of the information contained in this report, or that the use of any information, apparatus, method, or process disclosed in this report may not infringe privately owned rights; or

B. Assumes any liabilities with respect to the use of, or for damages resulting from the use of any information, apparatus, method, or process disclosed in this report.

As used in the above, "person acting on behalf of the Commission" includes any employee or contractor of the Commission, or employee of such contractor, to the extent that such employee or contractor of the Commission, or employee of such contractor prepares, disseminates, or provides access to, any information pursuant to his employment or contract with the Commission, or his employment with such contractor.

Addendum to ORNL-2831

The units on the curves of Fig. 3 through Fig. 26 were inadverently omitted. The density n_+ is in cm^{-3} and the current I is always in ma.

ORNL-2831

Contract No. W-7405-eng-26

Neutron Physics Division

CRITICAL CURRENT FOR BURNOUT IN AN OGRA-TYPE DEVICE

Albert Simon

Date Issued
OCT 23 1959

OAK RIDGE NATIONAL LABORATORY
Oak Ridge, Tennessee
operated by
UNION CARBIDE CORPORATION
for the
U.S. ATOMIC ENERGY COMMISSION

MARTIN MARIETTA ENERGY SYSTEMS LIBRARIES
3 4456 0361461 2

ABSTRACT

A complete algebraic analysis has been obtained for the variation of the steady state ion density n_+ with injected current I in an OGRA-type fusion device (i.e., a device based on trapping of ions by breakup of energetic molecular ions on collision with either the background gas or trapped ions). The most general variation of n_+ with I is shown to be an s-curve with at most three roots of n_+ for a given input I. A physical interpretation of these three roots is given. In addition algebraic expressions are obtained for the two currents at which the bends in the s-curve occur. It will be necessary to attain the larger current in order to build up a high density plasma when the density is being increased from below. On the other hand, once the high density has been achieved it may be maintained by steady injection of a current larger than the lower value. Parameters corresponding roughly to the specifications of OGRA are used to obtain some numerical results. In the final appendix, the previously published formulas for burnout in DCX are extended to include effects of neutral backstreaming from the input beam and "ion-pumping."

TABLE OF CONTENTS

		Page No.
	Abstract	iii
I.	Steady State Relation Between Ion Density and Injected Current	1
II.	The Injected Current as a Function of the Ion Density	6
III.	The Ion Density as a Function of the Injected Current	7
IV.	Physical Interpretation of the Roots	11
V.	The Upper Critical Current (UCC)	12
VI.	The Lower Critical Current (LCC)	15
VII.	Numerical Solutions for "OGRA"	16
VIII.	Summary	18
App. A.	The Path Length L Considered as a Fixed Range	44
App. B.	Extension of the DCX Burnout Formula to Include Ion Pumping	45

I. STEADY STATE RELATION BETWEEN ION DENSITY AND INJECTED CURRENT

In two previous publications,[1-2] an expression was derived for the critical current at which formation of a plasma by high-energy injection will begin. This previous expression was for a case in which the trapping mechanism (although not specified in detail) was localized and did not depend on either the neutral gas in the device, the trapped ion density or the dimensions of the system. A trapping mechanism of this sort is provided by the arc in DCX.[3]

The situation is quite different in a proposed fusion device such as OGRA.[4] Here the injected molecular ions have a long mean-free-path L before they strike the injector snout and trapping occurs by virtue of the dissociation of the molecule on collision with either the background gas (cross section $\sigma_B^{\,o}$), the trapped ions ($\sigma_B^{\,+}$), or other molecular ions in transit ($\sigma_B^{\,2+}$). Nevertheless, one might suspect on physical grounds that a critical current also exists in this case and indeed such an expression has been found. The result is somewhat more complex than in the case of DCX because of a feedback which is inherent in the gas-breakup scheme. The onset of neutral burnout results in a reduction of the neutral breakup centers as well as an increase of the ion breakup centers and hence has a back effect on the input trapped current.

A complete algebraic analysis of the steady state equations has been achieved in the case when one can neglect the contribution of the molecular ions to burnout or to breakup of other molecules as compared to the effect of the trapped ions and the neutral gas. (This is a highly valid approximation in almost all cases of interest.) The total mean free path λ of the injected molecular ions is then:

$$\frac{1}{\lambda} = \frac{1}{L} + \hat{N}_o \sigma_B^{\,o} + n_+ \sigma_B^{\,+} \qquad (1)$$

1. A. Simon, The Phys. of Fluids, 1, 495 (1958).
2. A. Simon, The Phys. of Fluids, 2, 336 (1959).
3. C. F. Barnett et al., Proc. Second Geneva Conf. 31, 298 (1958).
4. I. V. Kurchatov, J. Nuc. Energy 8, 168 (1958).

where $\hat{N}_o$ is the average neutral density (atomic) external to the plasma region and n_+ is the trapped energetic ion density. (It has been assumed that the slow ions resulting from ionization of the neutrals in the plasma region contribute equally to breakup as do the neutrals themselves. The sum of the slow ion and neutral densities in the plasma interior should remain equal to the external neutral density even after burnout.) The probability that a molecule will break up after a path length x is then

$$p(x) = e^{-x/\lambda} \frac{dx}{\lambda_B} \tag{2}$$

where

$$\frac{1}{\lambda_B} = \hat{N}_o \sigma_B^{\,o} + n_+ \sigma_B^{\,+} \tag{3}$$

The percentage trapping is found by integrating Eq. (2) over all space. The result is

$$\% \text{ B.U.} = \frac{\lambda}{\lambda_B} = \frac{\hat{N}_o \sigma_B^{\,o} L + n_+ \sigma_B^{\,+} L}{1 + \hat{N}_o \sigma_B^{\,o} L + n_+ \sigma_B^{\,+} L} \tag{4}$$

The steady state rate of trapping of energetic ions is obtained by multiplying Eq. (4) by I, where I is the injected (number) current of molecular ions. It is assumed that trapping by dissociation of the molecular ion will dominate over trapping by actual ionization.

The trapped ions will be lost from the plasma in two ways. Either they undergo a charge exchange collision with a background gas atom or they scatter on each other and go out the mirrors. Since mirror loss will be negligible until well after burnout sets in, we ignore any contribution to mirror loss due to scattering of the ions against the neutral gas atoms. The average neutral density $\bar{n}_o$ in the plasma interior is simply related to the exterior neutral density $\hat{N}_o$.[2]

$$\bar{n}_o \cong \frac{\hat{N}_o}{1 + \frac{\bar{\ell}}{\lambda}} \tag{5}$$

$$= \frac{\hat{N}_o}{1 + \frac{\bar{\ell}\, v}{v_o}\, n_+ \sigma_d^+} \tag{6}$$

Here $\bar{\ell}$ is the mean chord length of the plasma volume and λ is the mean-free-path for destruction of a gas atom (by either ionization or charge exchange) as it enters the plasma. Equation (6) expresses this mean free path in terms of the properties of the ions. The quantity σ_d^+ represents the sum of the cross sections for ionization and charge exchange of an ion incident on a gas atom:

$$\sigma_d^+ = \sigma_i + \sigma_{cx} \tag{7}$$

The background gas has been assumed to be of the same species as the injected molecular ion (i.e., deuterium or hydrogen in all cases of interest). Hence a single ionization or charge exchange suffices to make it impotent. The average velocity of the gas atom is denoted by v_o and v is the ion velocity. Throughout this paper we assume that energy degredation processes are unimportant and that the ions remain at their initial energy until they are lost.

The steady state loss rate of ions by charge exchange follows immediately from Eq. (6). It is:

$$= \frac{\hat{N}_o n_+ \sigma_{cx} vV}{1 + \frac{\bar{\ell} v}{v_o}\, n_+ \sigma_d^+} \tag{8}$$

where V is the plasma volume. Finally, the mirror loss rate is assumed to be given by the usual binary expression,[5]

$$= n_+^2 \sigma_c v P V \tag{9}$$

where σ_c is the "effective 90-deg. Coulomb scattering cross section" by cumulative small angle scattering and P is the probability of an ion being in the loss cone after such a scattering. Combining Eqs. (4), (8), and (9), we have the following steady state equation for the ion density:

$$\frac{I}{V} \frac{\hat{N}_o \sigma_B^o L + n_+ \sigma_B^+ L}{1 + \hat{N}_o \sigma_B^o L + n_+ \sigma_B^+ L} = \frac{\hat{N}_o n_+ \sigma_{cx} v}{1 + \frac{\bar{\ell}_v}{v_o} n_+ \sigma_d^+} + n_+^2 \sigma_c v P \tag{10}$$

An expression for $\hat{N}_o$, the neutral density exterior to the plasma may be readily obtained by accounting for all the sources of gas. The background gas is assumed to come from a steady outgassing of the walls of the container and from backstreaming of neutrals resulting from the energetic ions and molecular ions which are injected and which finally strike the walls. We assume that a certain fraction Γ of the input molecular ion ultimately enter the vacuum region as neutral atoms. Of course this is a rather crude accounting and does not distinguish between the different re-entry probabilities of energetic ions and unbroken-up molecular ions which strike the wall. By conservation of atoms, we see that $\Gamma \leq 2$. The steady outgassing rate of the surface is denoted by $\alpha \bar{S}$ where $\bar{S}$ is the surface area of interest and α is the outgassing rate per unit area.

This influx of gas is balanced in two ways. First, neutrals are pumped off directly by external pumps acting on the system. If θ denotes the pumping speed of the external pumps, this loss rate is $\theta \hat{N}_o$. The second loss is due

5. R. F. Post, Proc. Second Geneva Conf. 31, 248 (1958).

to the "ion-pumping" action of the trapped plasma. Every neutral atom which enters the plasma volume and undergoes either an ionization or a charge exchange becomes a slow ion. This ion is trapped on a field line and rapidly moves out to the mirror regions. A large fraction of these slow ions may be permanently trapped and prevented from returning to the vacuum region, for instance by accelerating them into a titanium plate and continually evaporating new layers of titanium on that region. This is one possible form of "ion-pumping." Let σ denote the fractional probability that a slow ion does <u>not</u> return as a neutral. The rate of loss of neutrals by this mechanism is then:

$$= \sigma \frac{\hat{N}_o n_+ \sigma_d^+ v}{1 + \frac{\bar{\ell} v}{v_o} n_+ \sigma_d^+} V$$

The resultant steady state equation for $\hat{N}_o$ is then:

$$\Gamma I + \alpha \bar{S} = \theta \hat{N}_o + \frac{\sigma \hat{N}_o n_+ \sigma_d^+ v V}{1 + \frac{\bar{\ell} v}{v_o} n_+ \sigma_d^+} \tag{11}$$

Now initially, in the absence of any input beam, the balance equation was

$$\alpha \bar{S} = \theta N_o \tag{12}$$

where N_o is the initial neutral density in the vacuum region before injection began. Substituting Eq. (12) in Eq. (11), we have

$$\hat{N}_o = \frac{\frac{\Gamma}{\theta} I + N_o}{1 + \frac{\sigma}{\theta} \frac{n_+ \sigma_d^+ v V}{1 + \frac{\bar{\ell} v}{v_o} n_+ \sigma_d^+}} \tag{13}$$

Equations (10) and (13) combined constitute an implicit equation in the variables n_+ and I. (Some of these last considerations on backstreaming and ion pumping have not been included in previous publications[1,2] on burnout in DCX. This is done here in Appendix B.)

II. THE INJECTED CURRENT AS A FUNCTION OF THE ION DENSITY

We wish to determine the variation of ion density n_+ with changes in the injected current I. The gross features of the variation may be obtained by an algebraic analysis. Equations (10) and (13) combined have the general form:

$$f(n_+, I) = 0 \tag{14}$$

Let us first determine the possible roots of this equation for fixed n_+.

We shall rewrite Eq. (14) so as to explicitly display it as a polynomial in I. From Eq. (10) we have:

$$\frac{I}{V}\left(\hat{N}_o \sigma_B^{\,o} L + n_+ \sigma_B^{\,+} L\right) = \left[\frac{\hat{N}_o n_+ \sigma_{cx} v}{1 + \frac{\bar{\ell} v}{v_o} n_+ \sigma_d^{\,+}} + n_+^{\,2} \sigma_c v P\right]\left[1 + \hat{N}_o \sigma_B^{\,o} L + n_+ \sigma_B^{\,+} L\right] \tag{15}$$

which has the general form, by Eq. (13),

$$\frac{I}{V}(AI + B) = (CI + D)(1 + AI + B) \tag{16}$$

where A, B, C, and D are positive definite quantities and are independent of I. Equation (16) may be written

$$I^2\left[\frac{A}{V} - AC\right] + I\left[\frac{B}{V} - C(1 + B) - AD\right] - D(1 + B) = 0 \tag{17}$$

Two cases may be distinguished:

a. $\frac{1}{V} > C$: In this case the product of the two roots is negative. Hence there is one positive real root and one negative real root.

b. $\frac{1}{V} < C$: The coefficient of I in Eq. (17) may be written as:

$$= B\left(\frac{1}{V} - C\right) - C - AD$$

Hence, in this case, it is negative. We see that the product of the roots is positive but that the sum of the roots is negative. This can only occur if the two roots are either both negative real or form a complex pair. There is no positive real root.

Hence, we see that there can be at most one positive real value of I for a given n_+.

III. THE ION DENSITY AS A FUNCTION OF THE INJECTED CURRENT

Let us now rewrite Eq. (15) in order to display it as a polynomial in n_+. We define the quantity K as,

$$K = \frac{\bar{\ell} v}{v_o} \sigma_d^+ + \frac{\sigma}{\theta} \sigma_d^+ vV, \tag{18}$$

and multiply through by $(1 + Kn_+)^2$ in Eq. (15). The result is:

$$\frac{I}{V}\left[\left(\frac{\Gamma}{\theta} I + N_o\right)\left(1 + \frac{\bar{\ell} v}{v_o}\sigma_d^+ n_+\right)\sigma_B^o L + n_+\sigma_B^+ L(1 + Kn_+)\right](1 + Kn_+) =$$

$$= \left[\left(\frac{\Gamma}{\theta} I + N_o\right) n_+\sigma_{cx} v + n_+^2 \sigma_c vP(1 + Kn_+)\right] \cdot \tag{19}$$

$$\left[(1 + n_+\sigma_B^+ L)(1 + Kn_+) + \left(\frac{\Gamma}{\theta} I + N_o\right)\sigma_B^o L\left(1 + \frac{\bar{\ell} v}{v_o} n_+\sigma_d^+\right)\right]$$

which has the general form:

$$An_+^5 - Bn_+^4 + Cn_+^3 - Dn_+^2 + En_+ - F = 0 \tag{20}$$

Here

$$A = \sigma_c vP \lambda^2 \sigma_B^+ L$$

$$B = -\sigma_c vP\lambda \left[\sigma_B^+ L + \lambda + \left(\frac{\Gamma}{\theta} I + N_o\right) \sigma_B^o L \frac{\bar{\ell}_v}{v_o} \sigma_d^+\right]$$

$$F = \frac{I}{V} \left(\frac{\Gamma}{\theta} I + N_o\right) \sigma_B^o L$$

We see immediately that the product of the roots is positive and that the sum of the roots is negative. It follows at once that there is either only one positive real root or three positive real roots for n_+ for a given value of I.

The results of Sections II and III enable us to sketch the general variation of n_+ with I and this is shown in Fig. 1. The curve has the general form of an s-curve.[6] It should be noted that the root analysis given above does not exclude the possibility that the s-curve behavior will occur several times instead of just once as shown in Fig. 1. The physical interpretation of the s-curve given in the next section makes it clear, however, that an s-curve will occur only once if at all. In this regard, it should be noted that in some cases no s-curve appears and instead the curve increases monotonically to a limiting value of n_+. The criterion for the occurence of this behavior is given below [see Eq. (32)].

For comparison, the characteristic curve of n_+ versus I in the case of a fixed breakup device such as DCX is shown in Fig. 2.

---

6. A recent paper by I. N. Golovin (Harwell, April 1959, unpublished) states that Kuznetsov and coworkers have numerical results indicating a behavior of this sort.

UNCLASSIFIED
ORNL-LR-DWG 39282

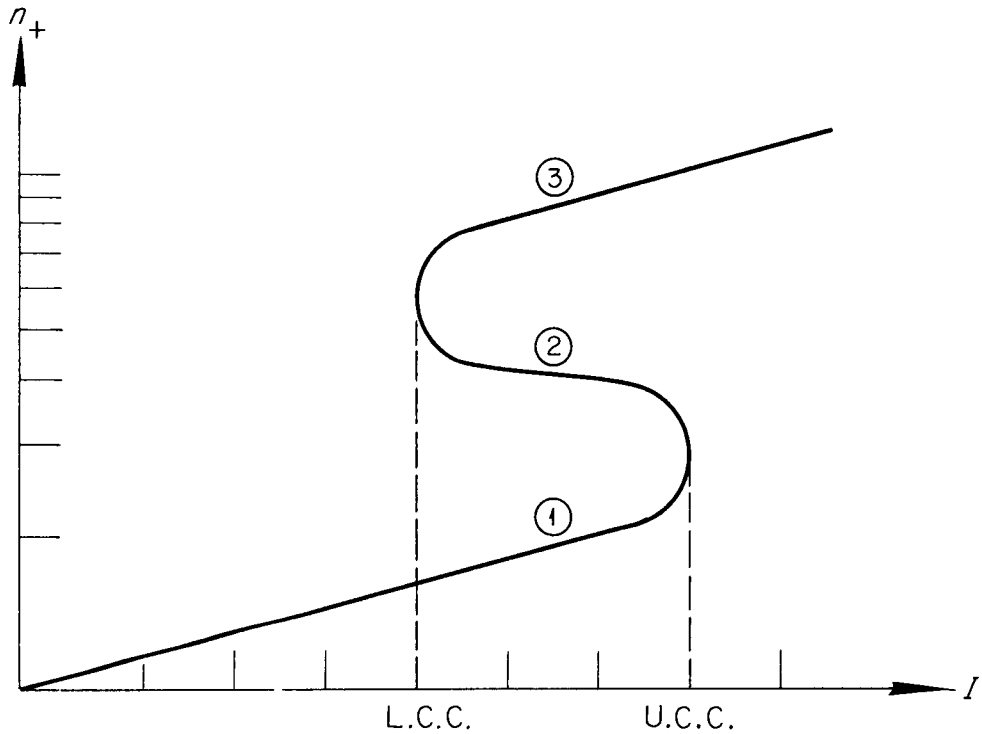

Fig. 1. Variation of Steady State Ion Density with Injected Current for an OGRA-Type Device.

UNCLASSIFIED
ORNL-LR-DWG 39283

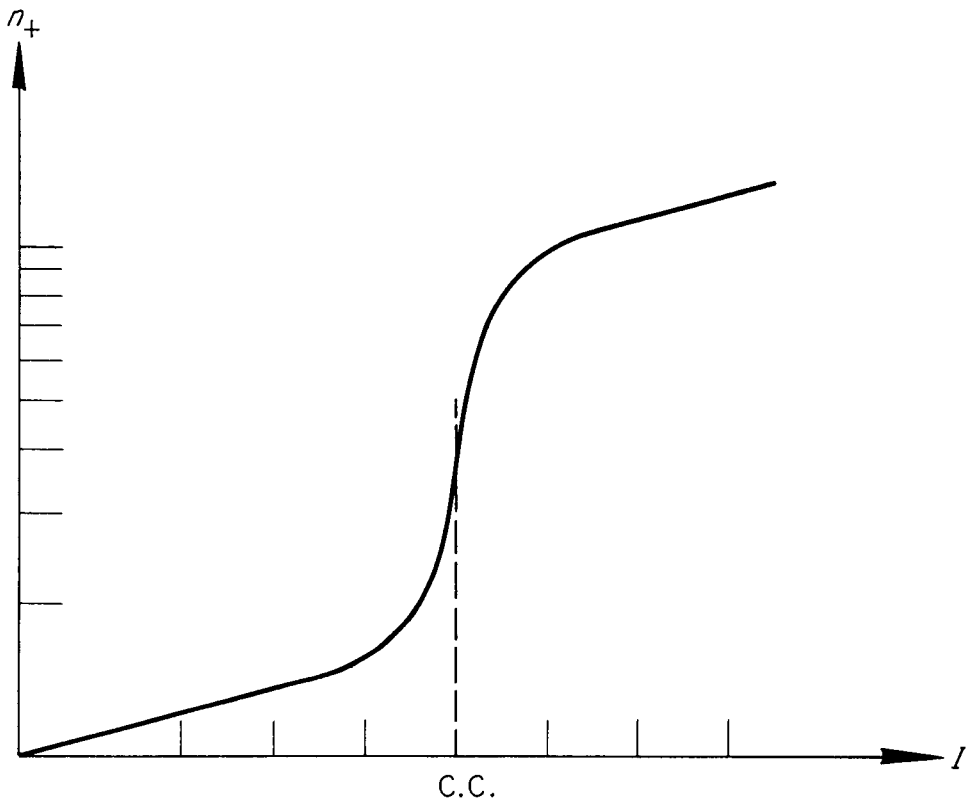

Fig. 2. Variation of Steady State Ion Density with Injected Current for a DCX-Type Device.

IV. PHYSICAL INTERPRETATION OF THE ROOTS

The multiple roots occurring in Fig. 1 have a straightforward physical interpretation. In region 1 neutral burnout has set in. The steady state solution is achieved by balance between charge exchange loss of the trapped ions and feed by breakup of the molecular ions on the neutral background (mirror loss is negligible). The second solution in region 2 corresponds to the point at which the ion density has risen and the neutral density has fallen such that the breakup on the ions now is the same as the previous breakup on the neutral gas. The charge exchange loss remains the same since it is proportional to the product $n_o n_+$ (where n_o is the average neutral density in the plasma region) and since, after burnout, $n_o \sim 1/n_+$. The final root of region 3 corresponds to the point at which mirror loss becomes more important than charge exchange loss.

The physical interpretation just given makes it clear that roots 1 and 3 are stable while root 2 is unstable. For example, suppose the system is in steady-state equilibrium at root 1 and that there is then a slight transient increase in the trapped ion density. The trapping rate will not increase appreciably since it is determined by the neutral gas density while the charge exchange loss rate increases linearly with n_+. Hence the ion density will decrease and this root is stable. If the system is in equilibrium at root 2, the reaction to this increase is quite different. The trapping rate increases linearly with n_+ since trapping is now primarily by collision with ions while the charge exchange loss rate (beyond burnout) remains constant. Hence the ion density will continue to increase and the root is unstable. Finally consider the effect of a transient increase at root 3. The trapping rate increases linearly but the dominant mirror loss rate increases quadratically. Hence the ion density decreases and this root is stable.

V. THE UPPER CRITICAL CURRENT (UCC)

Of course we can stop at this point and analyze the behavior of any given device by obtaining a curve such as in Fig. 1 from Eqs. (10) and (13) by numerical means. This is somewhat laborious, particularly if we wish to do a parameter survey and compare various proposals. Instead of the entire curve in Fig. 1, it would be almost as useful to know the two points at which the curve is vertical. These are denoted as the Upper Critical Current (UCC) and Lower Critical Current (LCC) in Fig. 1. It is clear that it is necessary to attain the UCC in order to build up a high density plasma when the density is being increased from below. On the other hand, once a high density has been achieved, it may be maintained by steady injection of a current larger than the LCC. A derivation of an approximate expression for the UCC is given below and one for the LCC is given in the next section.

Let us consider I as a function of n_+ and differentiate Eq. (14). We have:

$$\frac{\partial f}{\partial n_+} + \frac{dI}{dn_+} \frac{\partial f}{\partial I} = 0 \tag{21}$$

Now the UCC and LCC are distinguished by being the points at which $dI/dn_+ = 0$. Hence we have

$$\frac{\partial f}{\partial n_+} = 0 \tag{22}$$

The UCC and LCC are determined by the simultaneous solution of Eqs. (14) and (22). Substituting in Eq. (22) from Eq. (10), we have

$$\frac{\partial}{\partial n_+}\left[\frac{I}{V}\,\frac{\hat{N}_o\sigma_B{}^oL + n_+\sigma_B{}^+L}{1 + \hat{N}_o\sigma_B{}^oL + n_+\sigma_B{}^+L}\right] = \frac{\partial}{\partial n_+}\left[\frac{\hat{N}_o n_+\sigma_{cx}v}{1 + \frac{\bar{\ell}v}{v_o}\,n_+\sigma_d{}^+} + n_+{}^2\sigma_c vP\right]$$

$$= \frac{\partial}{\partial n_+}\left[\frac{\left(\frac{\Gamma}{\theta}\,I + N_o\right)n_+\sigma_{cx}v}{1 + \mathcal{K}n_+} + n_+{}^2\sigma_c vP\right] \qquad (23)$$

where $\mathcal{K}$ is defined in Eq. (18).

To get an expression for the UCC we neglect the second term on the right side of Eq. (23). This corresponds to mirror loss and should be negligible according to the physical interpretation given earlier. To get a relatively simple result we must make one other approximation. We assume that the UCC is well above burnout, or in other words, that $\mathcal{K}n_+ >> 1$ at that point. To first approximation, then, the bracket on the right hand side of Eq. (23) is independent of n_+ and its partial derivative vanishes. Equation (23) becomes

$$\frac{\partial}{\partial n_+}\left[\frac{\hat{N}_o\sigma_B{}^oL + n_+\sigma_B{}^+L}{1 + \hat{N}_o\sigma_B{}^oL + n_+\sigma_B{}^+L}\right] = 0 \qquad (24)$$

Now

$$\frac{d}{dx}\left(\frac{y}{1 + y}\right) = \frac{\frac{dy}{dx}}{(1 + y)^2} \qquad (25)$$

Hence Eq. (24) reduces to

$$\frac{\partial}{\partial n_+}\left(\hat{N}_o\sigma_B{}^oL + n_+\sigma_B{}^+L\right) = 0 \qquad (26)$$

or

$$\frac{\partial}{\partial n_+}\left[\frac{\left(\frac{\Gamma}{\theta} I + N_o\right)\sigma_B{}^o L\left(1 + \frac{\bar{\ell}_v}{v_o} n_+\sigma_d{}^+\right)}{(1 + \mathcal{K} n_+)} + n_+\sigma_B{}^+ L\right] = 0 \tag{27}$$

After some algebra, this equation reduces to:

$$(1 + \mathcal{K} n_+) = \sqrt{\frac{\left(\frac{\Gamma}{\theta} I + N_o\right)\sigma_B{}^o}{\sigma_B{}^+}\left(\frac{\sigma}{\theta}\right)\sigma_d{}^+ vV \equiv \phi} \tag{28}$$

or

$$n_+ = \frac{\phi - 1}{\mathcal{K}} \tag{29}$$

We can now eliminate n_+ in Eq. (14) by use of Eq. (29). The result is an implicit equation in I, whose solution should be the UCC. This equation is easily found to be:

$$I = \frac{\left(\frac{\Gamma}{\theta} I + N_o\right)\sigma_{cx} vV\left(\frac{\phi - 1}{\phi}\right)\left[1 + \Lambda\sigma_B{}^o L\left(\frac{\phi - 1}{\mathcal{K}}\right)\sigma_B{}^+ L\right.}{\mathcal{K}\left[\Lambda\sigma_B{}^o L + \left(\frac{\phi - 1}{\mathcal{K}}\right)\sigma_B{}^+ L\right]} \tag{30}$$

where

$$\Lambda = \left(\frac{\Gamma}{\theta} I + N_o\right)\left[1 + \left(\frac{\phi - 1}{\mathcal{K}}\right)\frac{\bar{\ell}_v}{v_o}\sigma_d{}^+\right]\frac{1}{\phi} \tag{31}$$

The solution of Eq. (30) gives us the UCC and the corresponding value of n_+ is then given by Eq. (29).

It should be noted that we assumed initially that $\mathcal{K} n_+ >> 1$ at the UCC. In order to be self-consistent, then, the value of ϕ corresponding to our solution should be large compared to unity. Our numerical results seem to

indicate that quite good answers are obtained for the UCC even when ϕ is of the order of 2. When ϕ is less than unity, the approximation breaks down completely and in this case we have found no simple relation which can be used.

It has not yet been demonstrated that there is only one real positive value of I which satisfies Eq. (30). We have succeeded in showing this in the limit of $\phi >> 1$. The method is similar to that used earlier and consists in expressing Eq. (30) as a (3rd order) polynomial in ϕ. It can be shown that one positive real solution for ϕ exists if

$$\frac{\theta \bar{\ell}}{V v_o} + \sigma > \Gamma \frac{\sigma_{cx}}{\sigma_d^+} \tag{32}$$

If the inequality is reversed, there is no positive real root. From the definition of ϕ, Eq. (28), we see that Eq. (32) is a necessary condition for the existance of an UCC.

One final point before leaving this section. If we make the opposite assumption to that made at the beginning of this section and take $\kappa n_+ << 1$, it is then easy to show that no simultaneous solution of Eqs. (23) and (14) can exist. This verifies our physical understanding of the roots which requires that burnout occur in order that an UCC exist.

VI. THE LOWER CRITICAL CURRENT (LCC)

The LCC is determined by the simultaneous solution of Eqs. (23) and (14). Our previous physical picture of conditions at the LCC indicated that the neutral background should be entirely negligible at that point. Hence we neglect the terms $\hat{N}_o \sigma_B^o L$ compared to $n_+ \sigma_B^+ L$ in Eq. (23). Correspondingly we assume that $n_+ \sigma_B^+ L >> 1$ and $\kappa n_+ >> 1$. Equation (23) becomes:

$$\frac{\partial}{\partial n_+}\left[\frac{I}{V}\left(1 - \frac{1}{n_+ \sigma_B^+ L}\right)\right] = \frac{\partial}{\partial n_+}\left[\frac{\left(\frac{\Gamma}{\theta} I + N_o\right)\sigma_{cx} v}{\kappa}\left(1 - \frac{1}{\kappa n_+}\right) + n_+^2 \sigma_c v P\right] \tag{33}$$

The solution of this equation is:

$$n_+^3 = \frac{1}{2\sigma_c vP} \left[\frac{I}{V\sigma_B^+ L} - \frac{\left(\frac{\Gamma}{\theta} I + N_o\right) \sigma_{cx} v}{K^2} \right] \tag{34}$$

which can be rewritten by use of Eq. (14) as:

$$n_+ = \left\{ \frac{1}{3\sigma_c vP} \left[\frac{I}{V} - \frac{\left(\frac{\Gamma}{\theta} I + N_o\right) \sigma_{cx} v}{K} \right] \right\}^{\frac{1}{2}} \equiv \delta \tag{35}$$

Upon substitution in Eq. (14), we obtain an implicit equation in I,

$$I = \frac{\left(\frac{\Gamma}{\theta} I + N_o\right) \sigma_{cx} vV \left(1 - \frac{3}{2K\delta}\right)}{K \left(1 - \frac{3}{2\delta\sigma_B^+ L}\right)} \tag{36}$$

Just as in the case of the UCC, this expression is self-consistent only if the resulting solution is such that $K\delta >> 1$ and $\sigma_B^+ L\delta >> 1$. Once again, in this limit, it is immediately demonstrated that there is at most one real positive root of Eq. (36) and that this root exists only if the inequality of Eq. (32) is satisfied.

VII. NUMERICAL SOLUTIONS FOR "OGRA"

A series of numerical runs was made using parameters which should be roughly that of the "OGRA" experiment. These parameters were:

$L = 10^5$ cm.

$\bar{\ell} = 50$ cm.

$V = 2.35 \times 10^6$ cm^3.

$\theta = 4 \times 10^7$ liters/sec.

$P = 0.388$.

Both H_2^+ and D_2^+ injection was considered, each at an energy of 200 kev. Furthermore, since there appear to be some large differences in published values, two sets of cross sections were used. One set, hereafter denoted by USSR, was taken from the curves of Federenko as given in reference 4. The other set, hereafter denoted as USA, were based on Barnett's results[7] and the Bethe formula for the ionization cross section.[8] These cross sections (per gas atom) are tabulated below:

a. Deuterium:

$$v_o = 1.26 \times 10^5 \text{ cm/sec}$$
$$v = 3.12 \times 10^8 \text{ cm/sec}$$
$$\sigma_c \cong 2.6 \times 10^{-22} \text{ cm}^2$$

	USA	USSR
σ_B^o	5×10^{-17}	1.65×10^{-16}
σ_B^+	5×10^{-17}	1.65×10^{-16}
σ_{cx}	9×10^{-17}	7.5×10^{-17}
σ_d^+	3.02×10^{-16}	2.6×10^{-16}

b. Hydrogen:

$$V_o = 1.78 \times 10^5 \text{ cm/sec}$$
$$v = 4.4 \times 10^8 \text{ cm/sec}$$
$$\sigma_c = 2.6 \times 10^{-22} \text{ cm}^2$$

	USA	USSR
σ_B^o	5×10^{-17}	1.3×10^{-16}
σ_B^+	5×10^{-17}	1.3×10^{-16}
σ_{cx}	1.2×10^{-17}	3×10^{-18}
σ_d^+	1.32×10^{-16}	1.08×10^{-16}

7. C. F. Barnett and H. K. Reynolds, Phys. Rev. 108, 355 (1958).
8. N. F. Mott and H. S. W. Massey, The Theory of Atomic Collisions, Oxford (1949) p. 247.

Runs were made for a variety of values of the initial pressure N_o, as well as Γ and σ. These results are plotted in Figs. 15-26. In a few cases, exact solutions of Eqs. (10) and (13) were obtained. These are shown in Figs. 3-14 together with the values of UCC and LCC determined from Eqs. (30) and (36).

VIII. SUMMARY

It is shown that the general shape of the curve which plots steady-state ion density versus injected current is an s-curve (see Fig. 1) for a gas breakup trapping device such as OGRA. The actual curve may be calculated by numerical means by use of Eqs. (10) and (13). Approximate expressions are obtained for the two points at which the curve is vertical. The upper critical current (UCC) is the solution of the implicit Eqs. (30) and (31). The corresponding density is then calculated in Eq. (29). The lower critical current is the solution of the implicit Eqs. (36) and (35). The corresponding density is then given by Eq. (35). Burnout and the characteristic s-curve will only occur if the inequality of Eq. (32) is satisfied. If not, there is simply a monotonic increase of the density to a limiting value as the current increases indefinitely.

A physical interpretation of these roots is given in Section IV. A numerical survey of UCC and LCC for an experimental device having the dimensions of the Russian OGRA are presented in Figs. 3-26. Appendix A considers the effect of treating the path length L as a fixed range rather than a mean free path and Appendix B applies the ion pumping consideration to previous formulas for burnout in DCX.

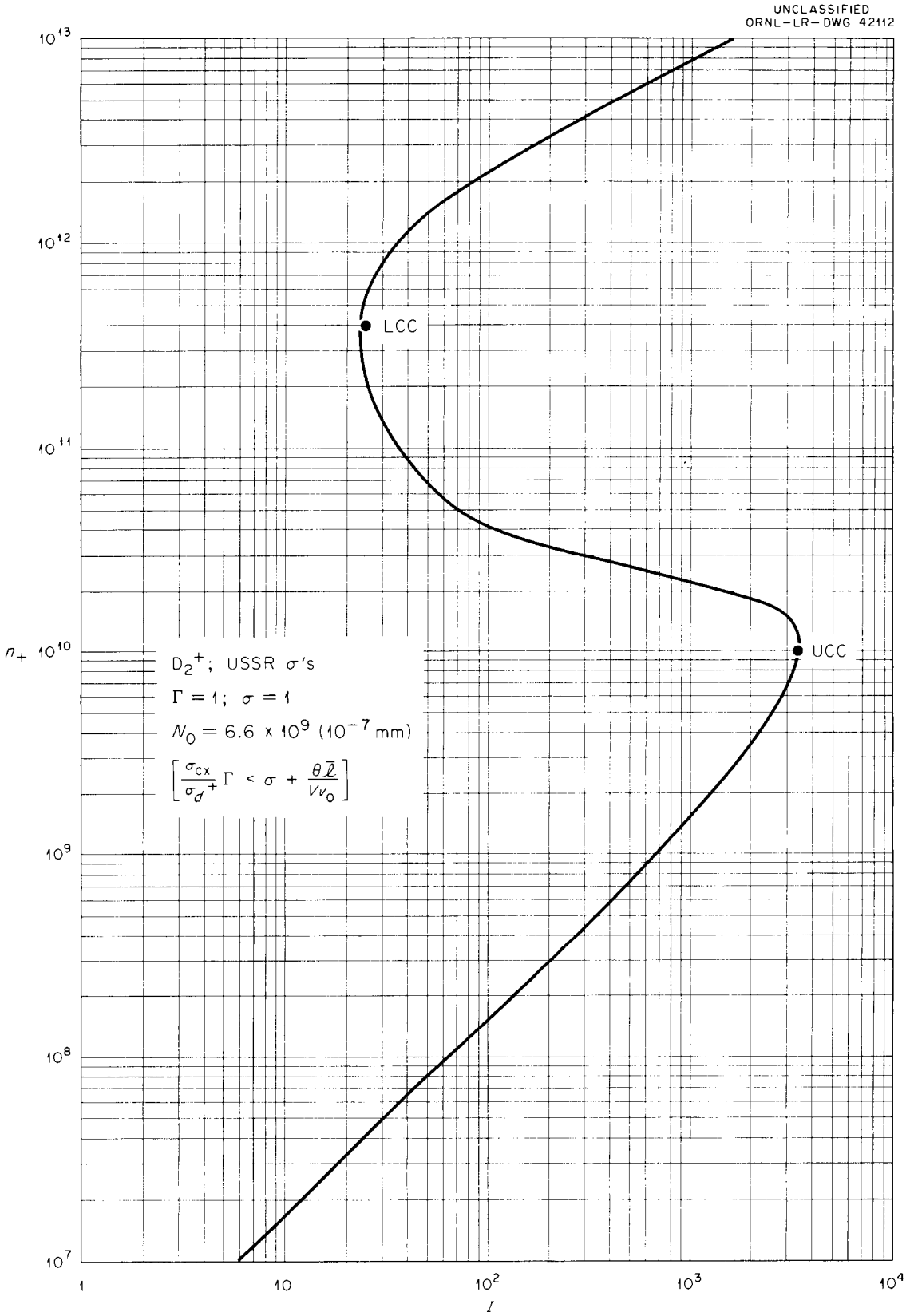
UNCLASSIFIED
ORNL-LR-DWG 42112
10^{13}
10^{12}
10^{11}
n_+ 10^{10}
10^{9}
10^{8}
10^{7}
1
10
10^2
10^3
10^4
I
LCC
UCC
D_2^+; USSR σ's
$\Gamma = 1$; $\sigma = 1$
$N_0 = 6.6 \times 10^9$ (10^{-7} mm)
$\left[\frac{\sigma_{cx}}{\sigma_d^+}\Gamma < \sigma + \frac{\theta \bar{\ell}}{V v_0}\right]$

Fig. 3.

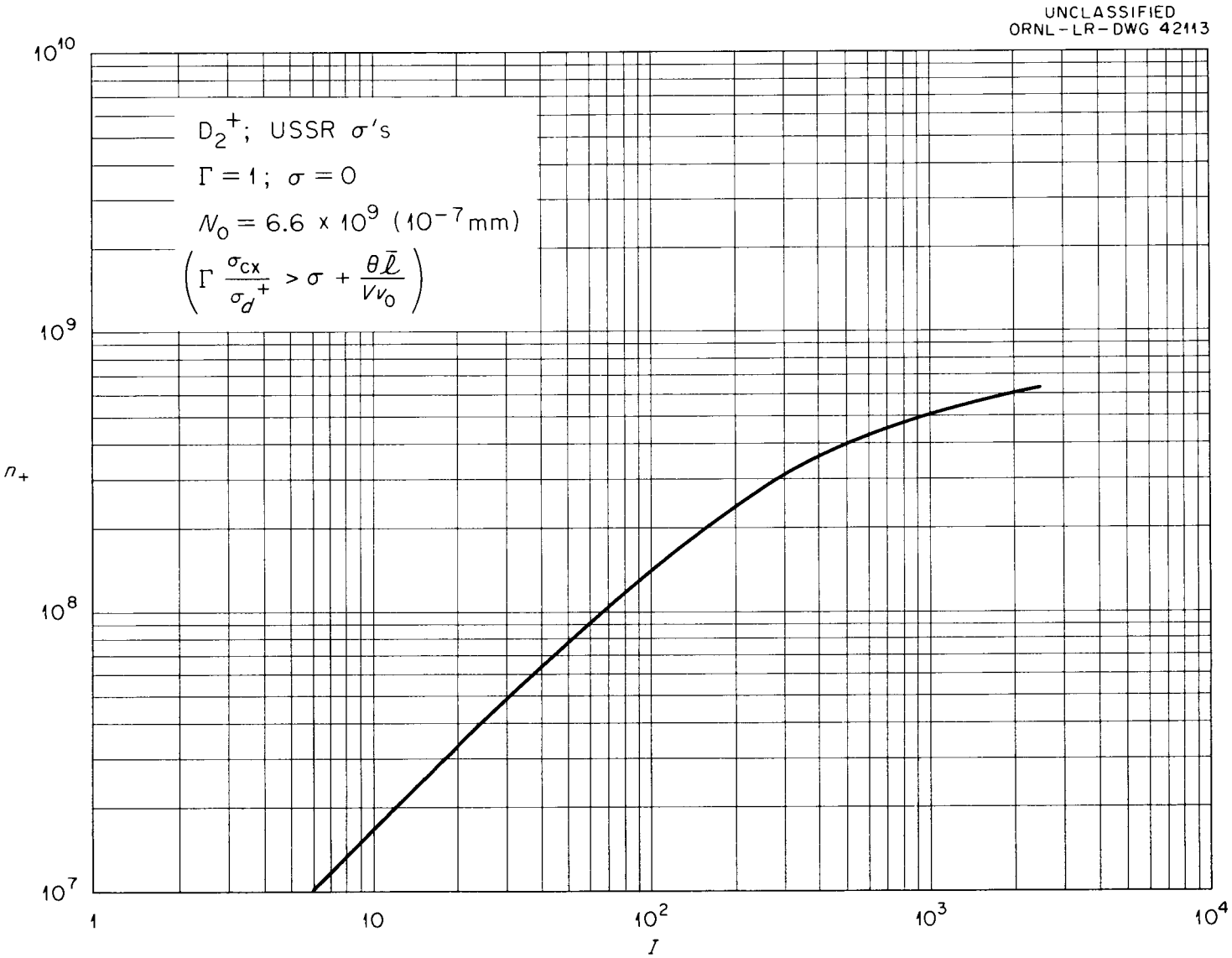
UNCLASSIFIED
ORNL-LR-DWG 42113
D_2^+; USSR σ's
$\Gamma = 1$; $\sigma = 0$
$N_0 = 6.6 \times 10^9$ (10^{-7} mm)
$\left(\Gamma \frac{\sigma_{cx}}{\sigma_{d^+}} > \sigma + \frac{\theta \bar{\ell}}{V v_0}\right)$
10^{10}
10^9
10^8
10^7
n_+
1
10
10^2
10^3
10^4
I

Fig. 4.

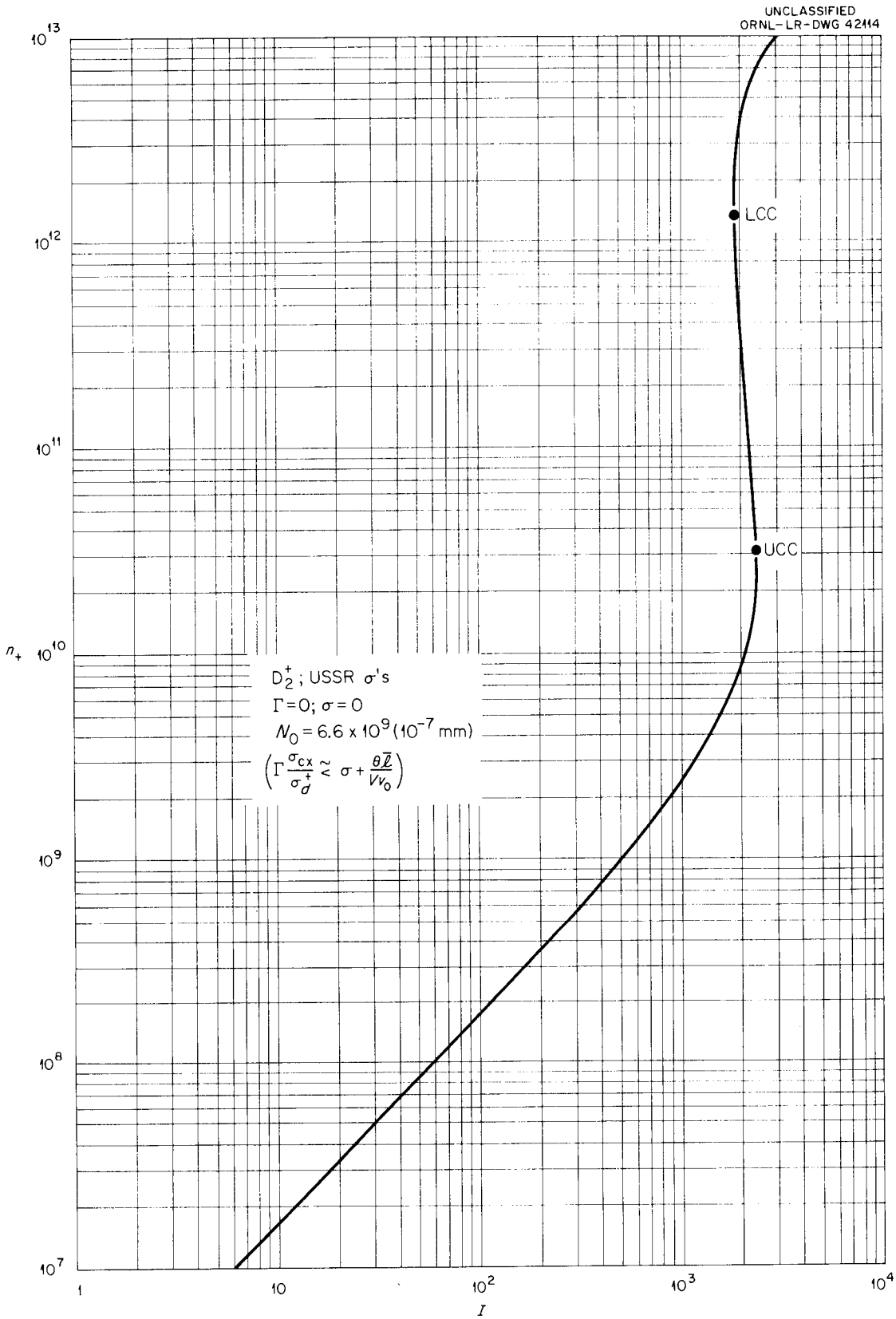
UNCLASSIFIED
ORNL-LR-DWG 42114
10^{13}
10^{12}
10^{11}
10^{10}
10^{9}
10^{8}
10^{7}
n_+
LCC
UCC
D_2^+; USSR σ's
$\Gamma = 0$; $\sigma = 0$
$N_0 = 6.6 \times 10^9 (10^{-7}$ mm)
$\left(\Gamma \frac{\sigma_{cx}}{\sigma_d^+} \lesssim \sigma + \frac{\theta \bar{l}}{V v_0}\right)$
1
10
10^2
10^3
10^4
I

Fig. 5.

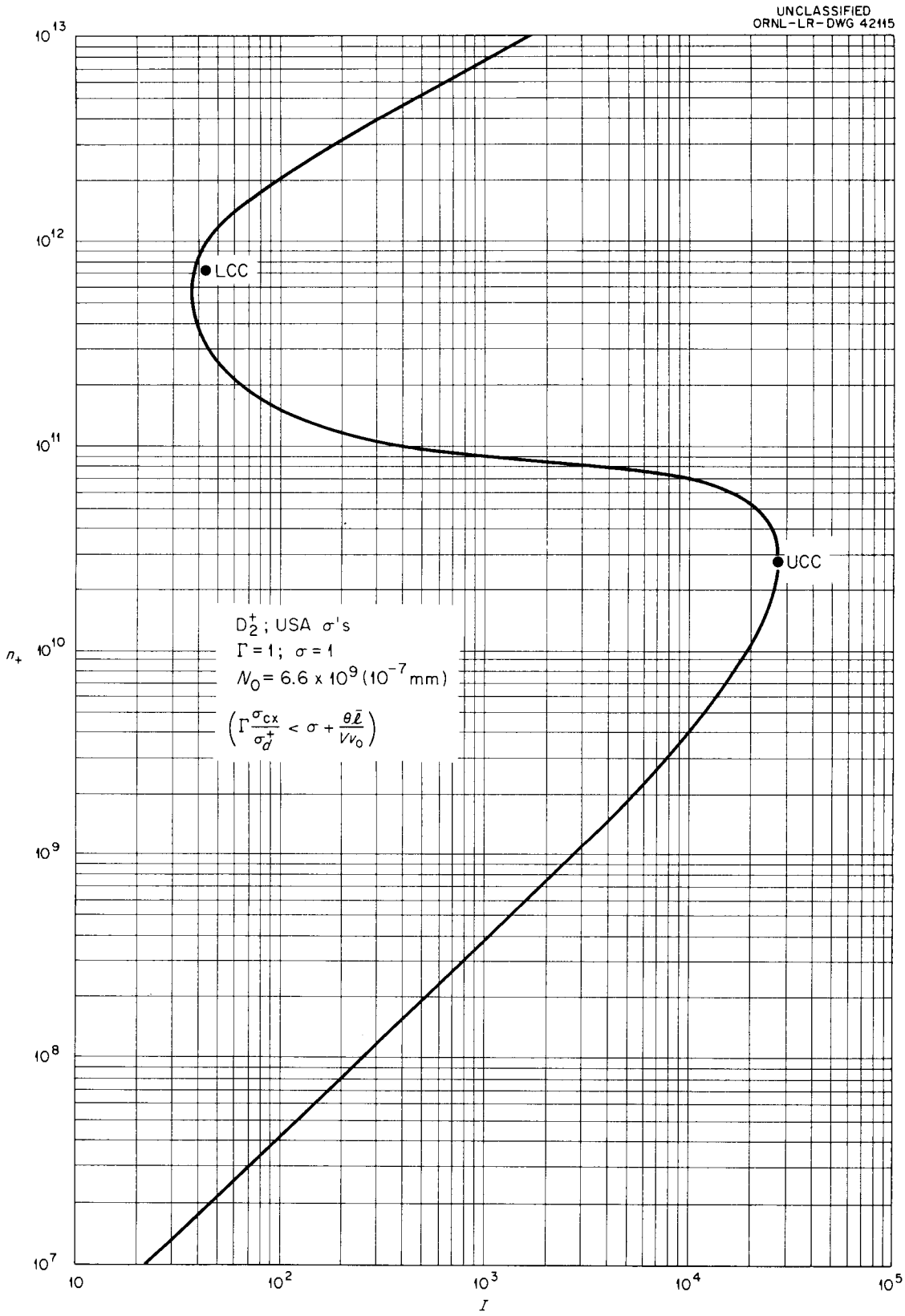
UNCLASSIFIED
ORNL-LR-DWG 42115
10^{13}
10^{12}
10^{11}
10^{10}
10^{9}
10^{8}
10^{7}
n_+
LCC
UCC
D_2^+; USA σ's
$\Gamma = 1$; $\sigma = 1$
$N_0 = 6.6 \times 10^9 (10^{-7}\,\mathrm{mm})$
$\left(\Gamma \frac{\sigma_{cx}}{\sigma_d^+} < \sigma + \frac{\theta \bar{\ell}}{V v_0}\right)$
10
10^2
10^3
10^4
10^5
I

Fig. 6.

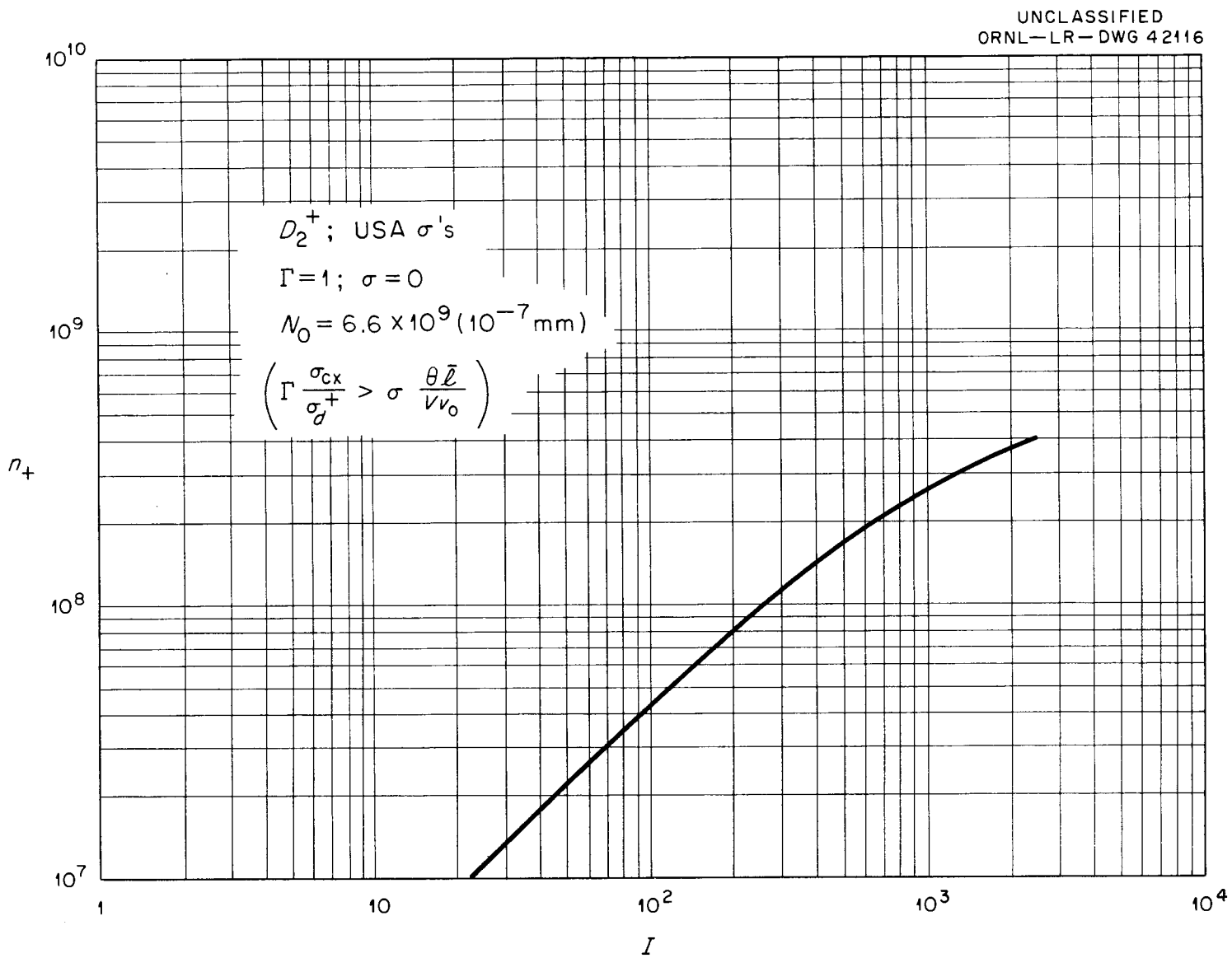
UNCLASSIFIED
ORNL—LR—DWG 42116
D_2^+; USA σ's
$\Gamma = 1$; $\sigma = 0$
$N_0 = 6.6 \times 10^9 (10^{-7}\,\mathrm{mm})$
$\left(\Gamma \frac{\sigma_{cx}}{\sigma_d^+} > \sigma \frac{\theta \bar{\ell}}{V v_0}\right)$
10^{10}
10^9
10^8
10^7
n_+
1
10
10^2
10^3
10^4
I

Fig. 7.

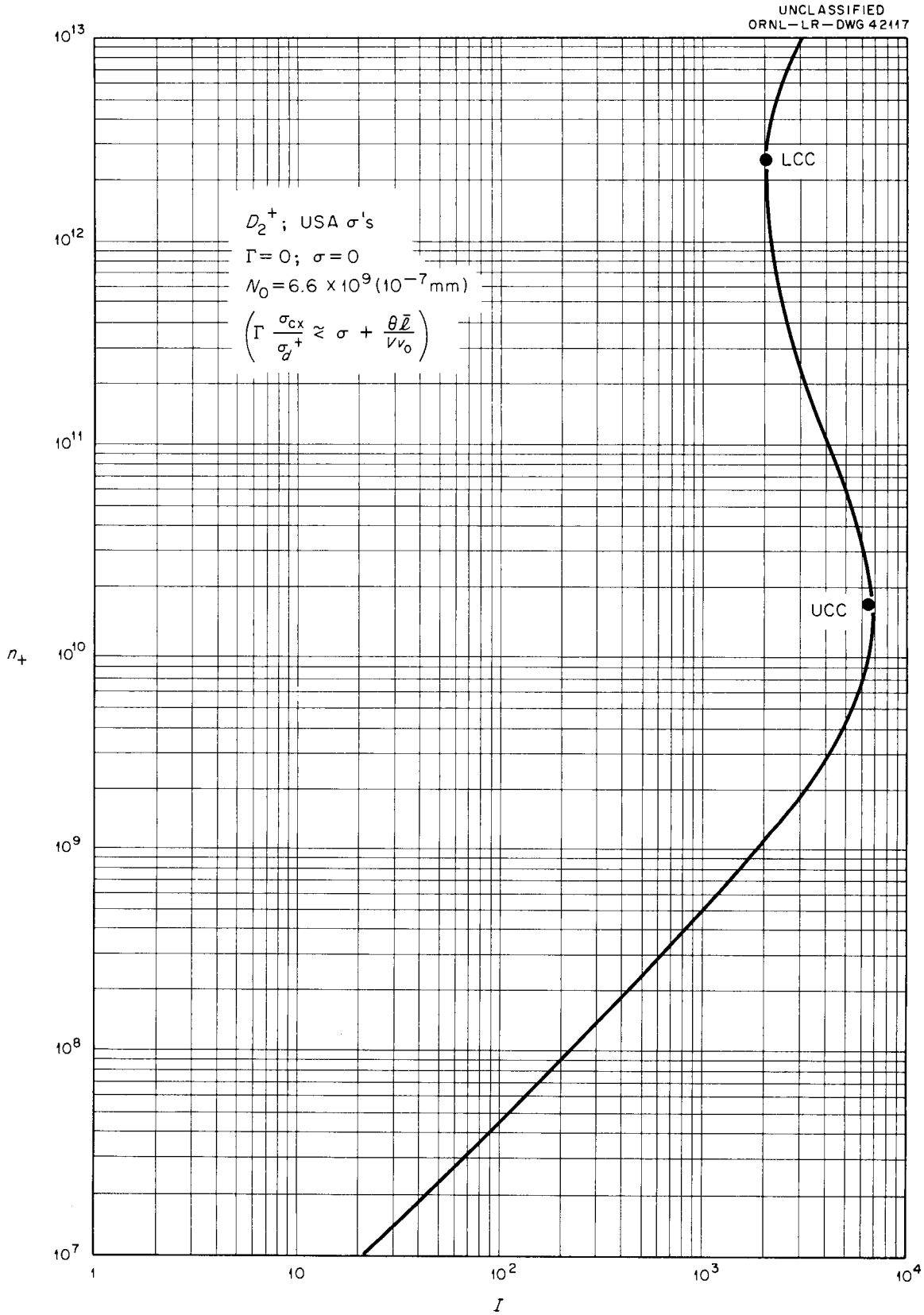
UNCLASSIFIED
ORNL–LR–DWG 42117
D_2^+; USA σ's
Γ = 0; σ = 0
$N_0 = 6.6 \times 10^9 (10^{-7}\,\mathrm{mm})$
$\left(\Gamma \frac{\sigma_{cx}}{\sigma_d^+} \gtrsim \sigma + \frac{\theta \bar{\ell}}{V v_0}\right)$
LCC
UCC
n_+
10^{13}
10^{12}
10^{11}
10^{10}
10^9
10^8
10^7
1
10
10^2
10^3
10^4
I

Fig. 8.

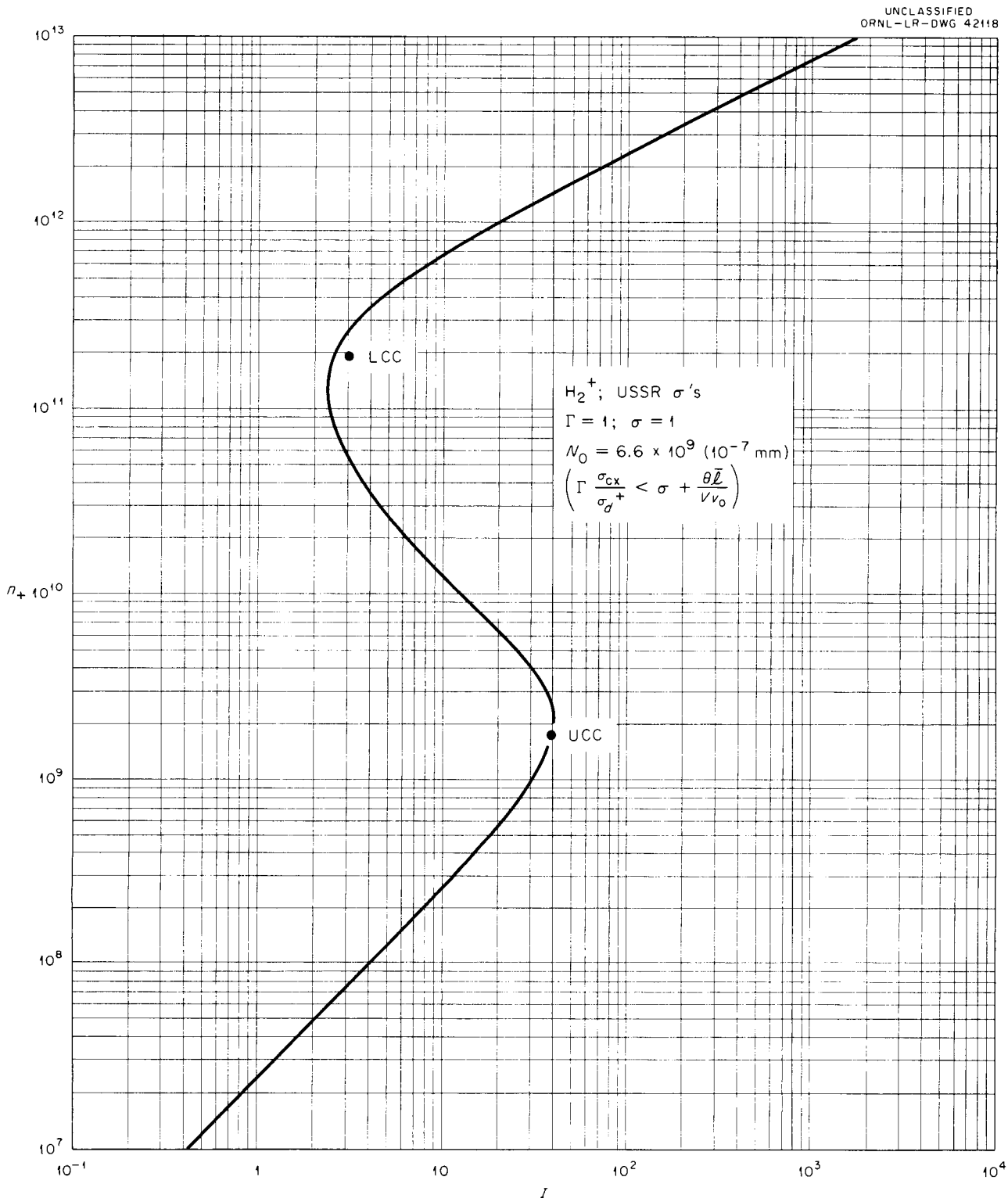
UNCLASSIFIED
ORNL-LR-DWG 42118
10^{13}
10^{12}
10^{11}
n_+ 10^{10}
10^{9}
10^{8}
10^{7}
10^{-1}
1
10
10^{2}
10^{3}
10^{4}
I
LCC
UCC
H_2^+; USSR σ's
$\Gamma = 1$; $\sigma = 1$
$N_0 = 6.6 \times 10^9$ (10^{-7} mm)
$\left(\Gamma \frac{\sigma_{cx}}{\sigma_d^+} < \sigma + \frac{\theta \bar{\ell}}{V v_0}\right)$

Fig. 9.

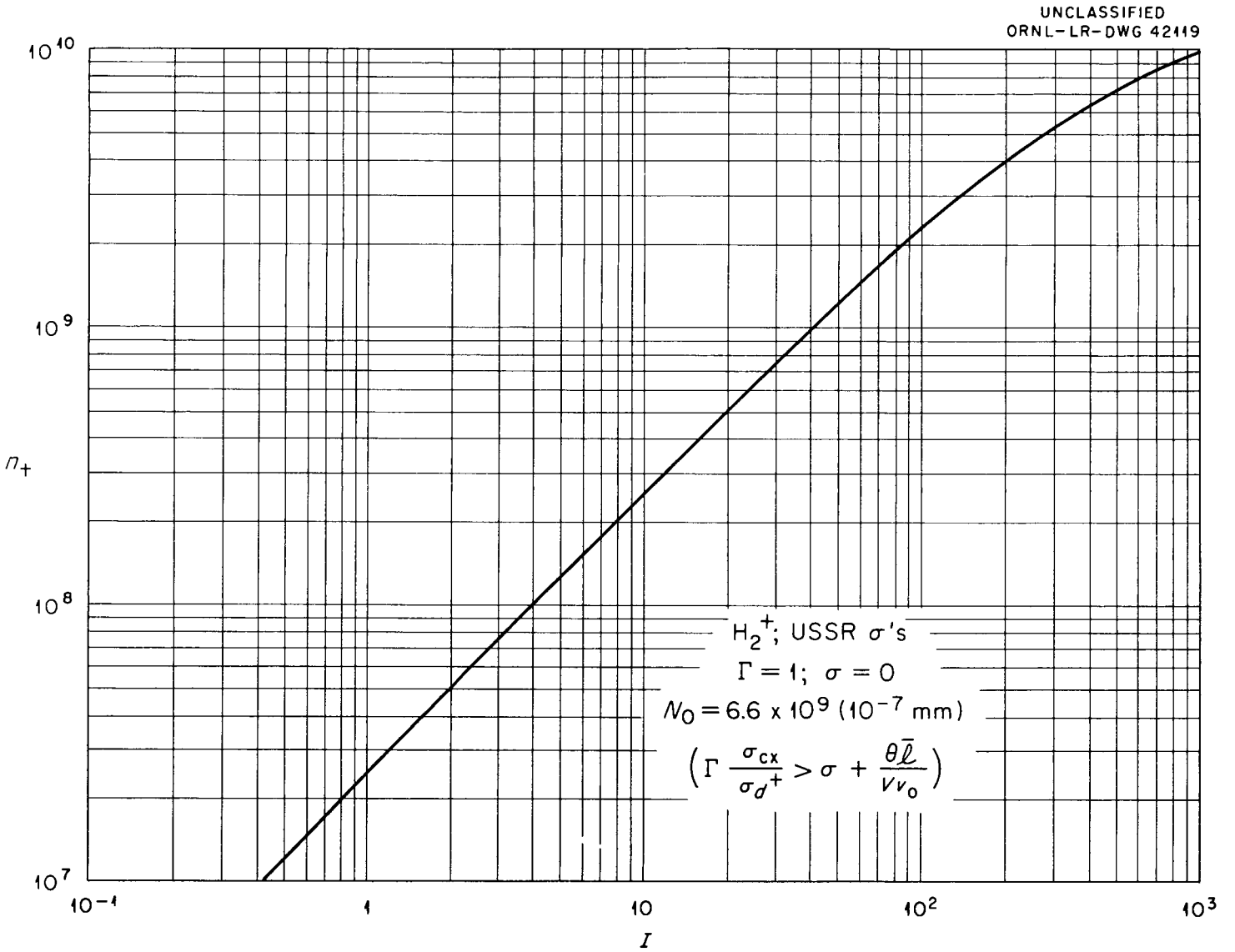
UNCLASSIFIED
ORNL-LR-DWG 42119
10^{10}
10^{9}
10^{8}
10^{7}
n_+
10^{-1}
1
10
10^2
10^3
I
H_2^+; USSR σ's
$\Gamma = 1$; $\sigma = 0$
$N_0 = 6.6 \times 10^9$ (10^{-7} mm)
$\left(\Gamma \frac{\sigma_{cx}}{\sigma_d^+} > \sigma + \frac{\theta \bar{\ell}}{V v_0}\right)$

Fig. 10.

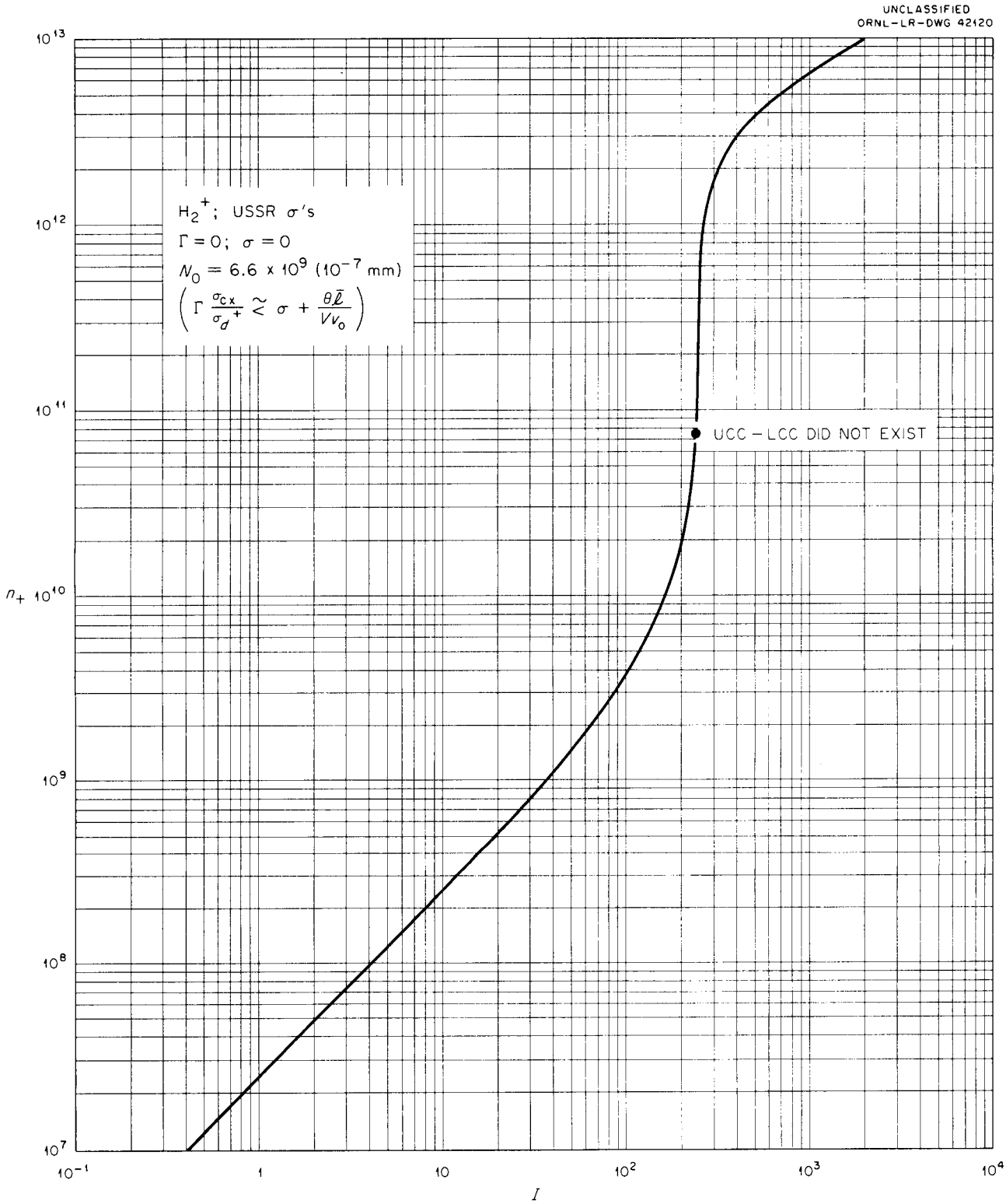
UNCLASSIFIED
ORNL-LR-DWG 42120
H_2^+; USSR σ's
$\Gamma = 0$; $\sigma = 0$
$N_0 = 6.6 \times 10^9$ (10^{-7} mm)
$\left(\Gamma \frac{\sigma_{cx}}{\sigma_d^+} \lesssim \sigma + \frac{\theta \bar{\ell}}{V v_0}\right)$
UCC – LCC DID NOT EXIST
n_+
10^{13}
10^{12}
10^{11}
10^{10}
10^9
10^8
10^7
10^{-1}
1
10
10^2
10^3
10^4
I

Fig. 11.

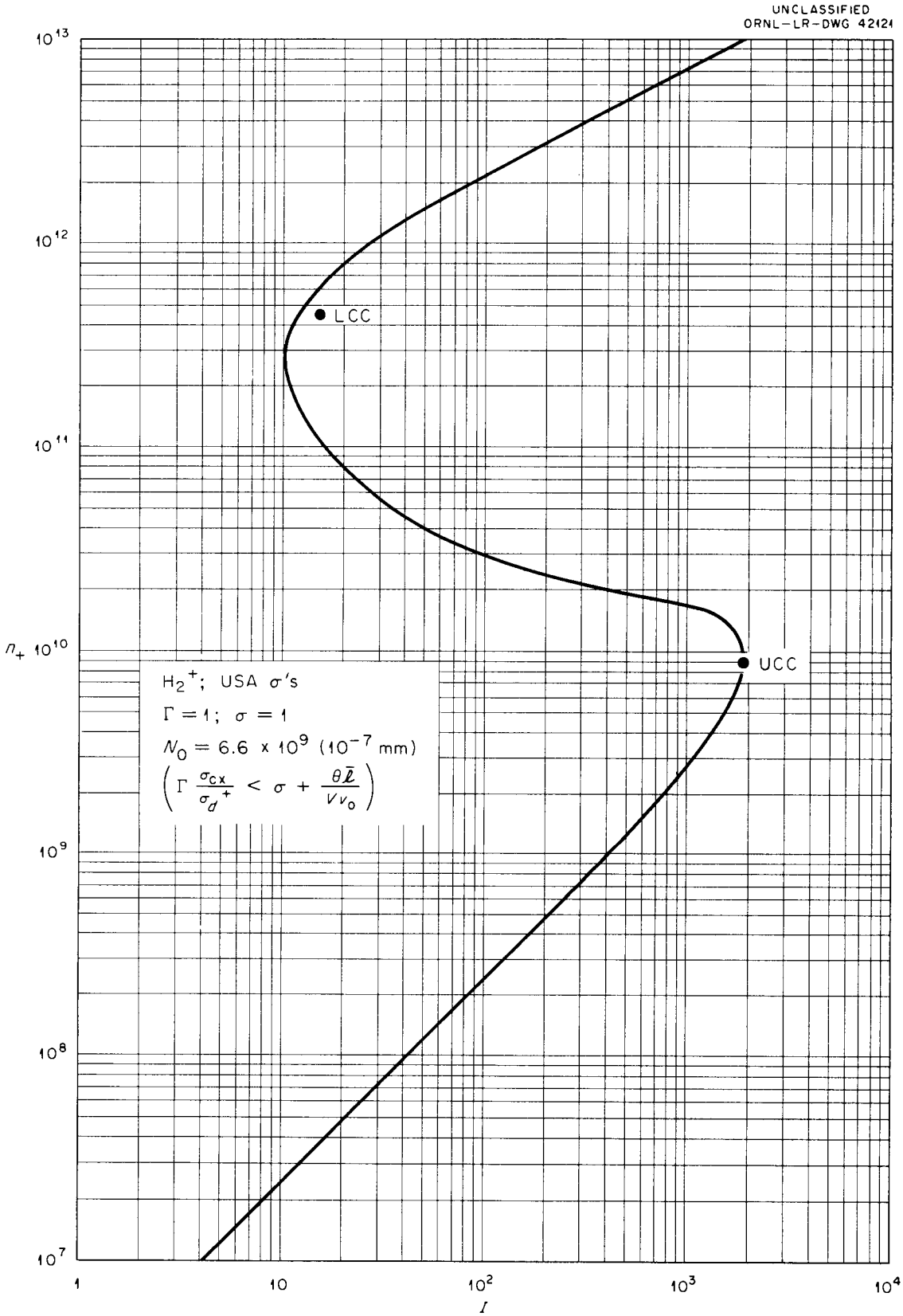
UNCLASSIFIED
ORNL-LR-DWG 42121
10^{13}
10^{12}
10^{11}
n_+ 10^{10}
10^{9}
10^{8}
10^{7}
1
10
10^2
10^3
10^4
I
LCC
UCC
H_2^+; USA σ's
$\Gamma = 1$; $\sigma = 1$
$N_0 = 6.6 \times 10^9$ (10^{-7} mm)
$\left(\Gamma \frac{\sigma_{cx}}{\sigma_d^+} < \sigma + \frac{\theta \bar{\ell}}{V v_0}\right)$

Fig. 12.

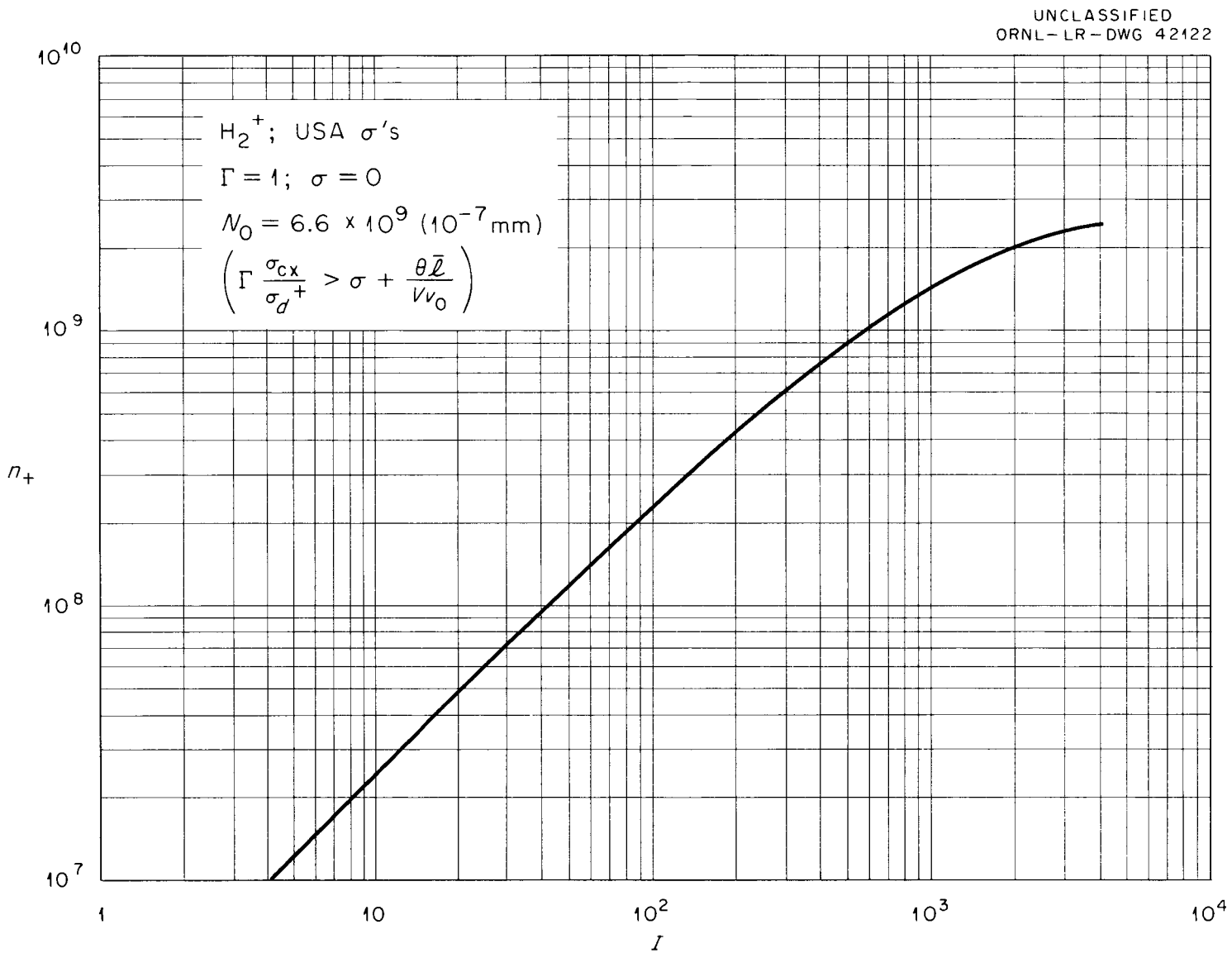
UNCLASSIFIED
ORNL-LR-DWG 42122
H_2^+; USA σ's
$\Gamma = 1$; $\sigma = 0$
$N_0 = 6.6 \times 10^9$ (10^{-7} mm)
$\left(\Gamma \frac{\sigma_{cx}}{\sigma_d^+} > \sigma + \frac{\theta \bar{\ell}}{V v_0}\right)$
10^{10}
10^9
10^8
10^7
n_+
1
10
10^2
10^3
10^4
I

Fig. 13.

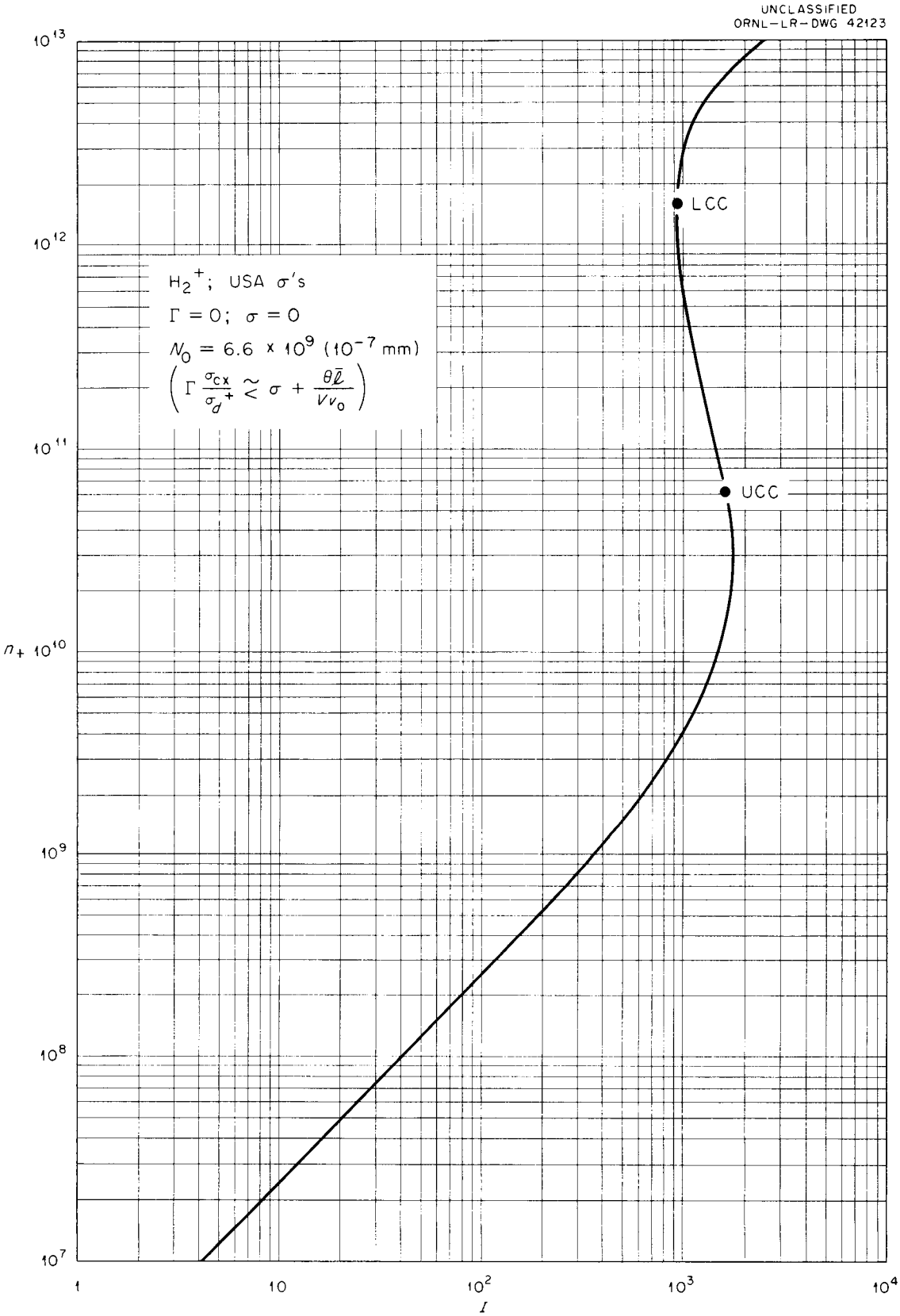
UNCLASSIFIED
ORNL-LR-DWG 42123
10^{13}
10^{12}
10^{11}
n_+ 10^{10}
10^9
10^8
10^7
1
10
10^2
10^3
10^4
I
LCC
UCC
H_2^+; USA σ's
$\Gamma = 0$; $\sigma = 0$
$N_0 = 6.6 \times 10^9$ (10^{-7} mm)
$\left(\Gamma \frac{\sigma_{cx}}{\sigma_d^+} \lesssim \sigma + \frac{\theta \bar{\ell}}{V v_0}\right)$

Fig. 14.

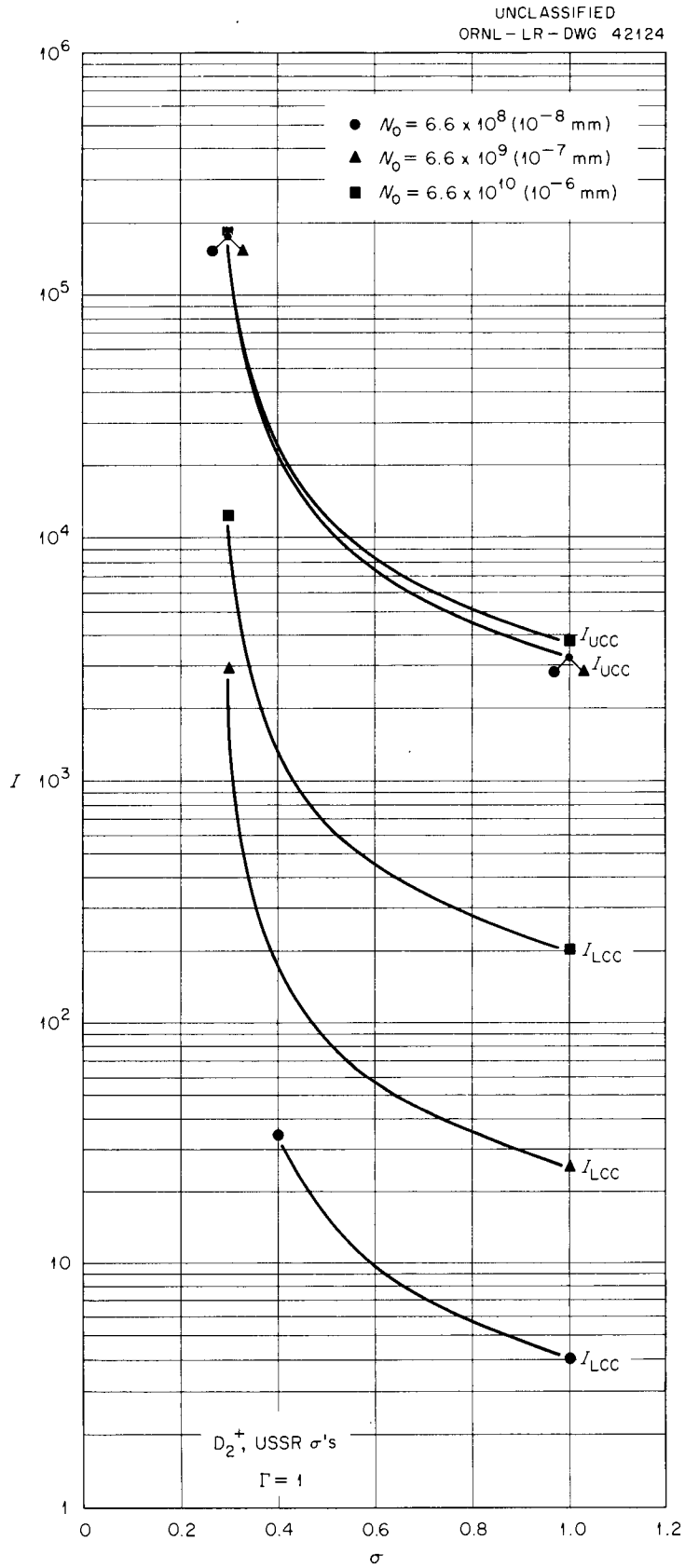
UNCLASSIFIED
ORNL - LR - DWG 42124
$N_0 = 6.6 \times 10^8$ (10^{-8} mm)
$N_0 = 6.6 \times 10^9$ (10^{-7} mm)
$N_0 = 6.6 \times 10^{10}$ (10^{-6} mm)
I_{UCC}
I_{UCC}
I_{LCC}
I_{LCC}
I_{LCC}
D_2^+, USSR σ's
$\Gamma = 1$
I
10^6
10^5
10^4
10^3
10^2
10
1
0
0.2
0.4
0.6
0.8
1.0
1.2
σ

Fig. 15.

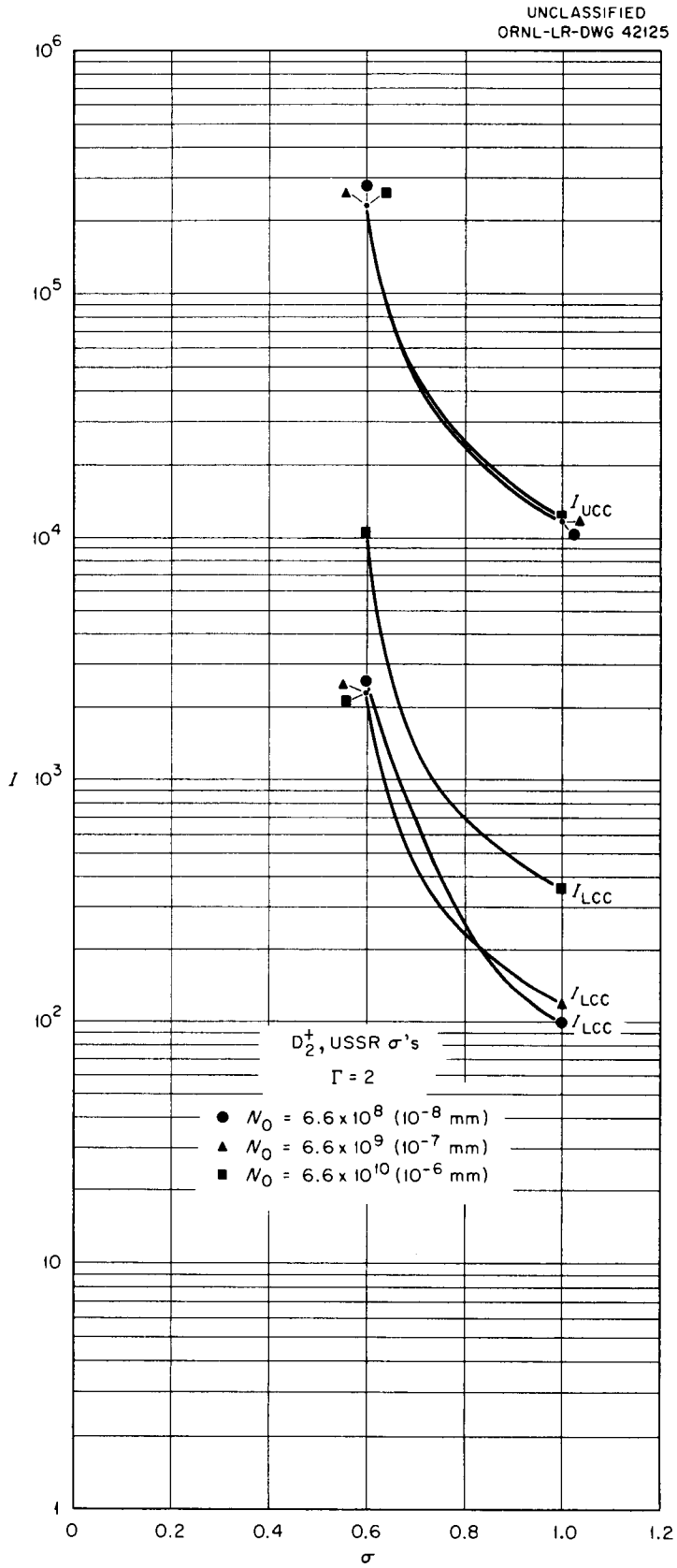
UNCLASSIFIED
ORNL-LR-DWG 42125
10^6
10^5
10^4
10^3
10^2
10
1
I
I_{UCC}
I_{LCC}
I_{LCC}
I_{LCC}
D_2^+, USSR σ's
$\Gamma = 2$
$N_0 = 6.6 \times 10^8$ (10^{-8} mm)
$N_0 = 6.6 \times 10^9$ (10^{-7} mm)
$N_0 = 6.6 \times 10^{10}$ (10^{-6} mm)
0
0.2
0.4
0.6
0.8
1.0
1.2
σ

Fig. 16.

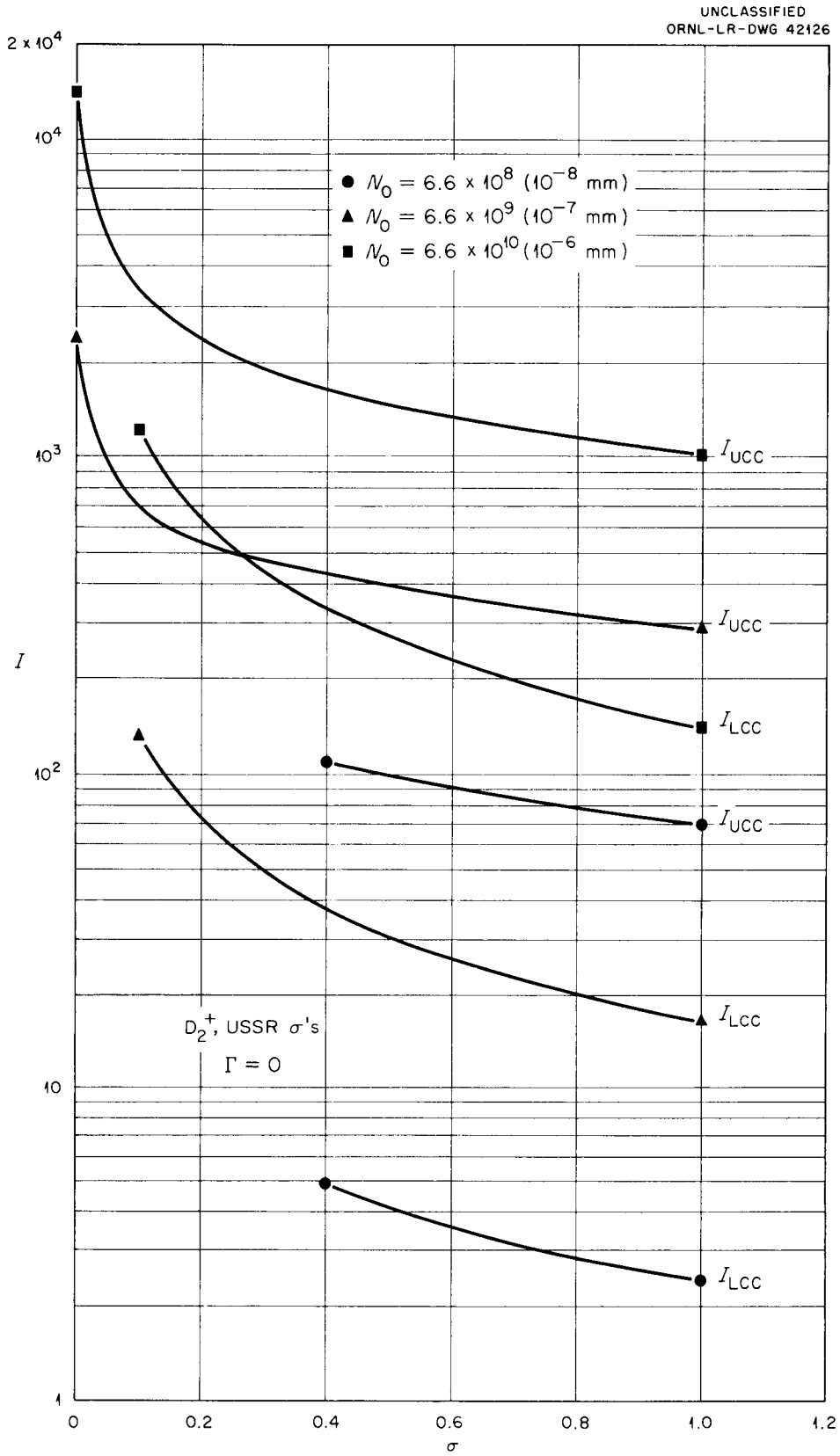
UNCLASSIFIED
ORNL-LR-DWG 42126
2 x 10^4
10^4
10^3
10^2
10
1
I
0
0.2
0.4
0.6
0.8
1.0
1.2
σ
● N0 = 6.6 x 10^8 (10^-8 mm)
▲ N0 = 6.6 x 10^9 (10^-7 mm)
■ N0 = 6.6 x 10^10 (10^-6 mm)
I_UCC
I_UCC
I_LCC
I_UCC
I_LCC
I_LCC
D2+, USSR σ's
Γ = 0

Fig. 17.

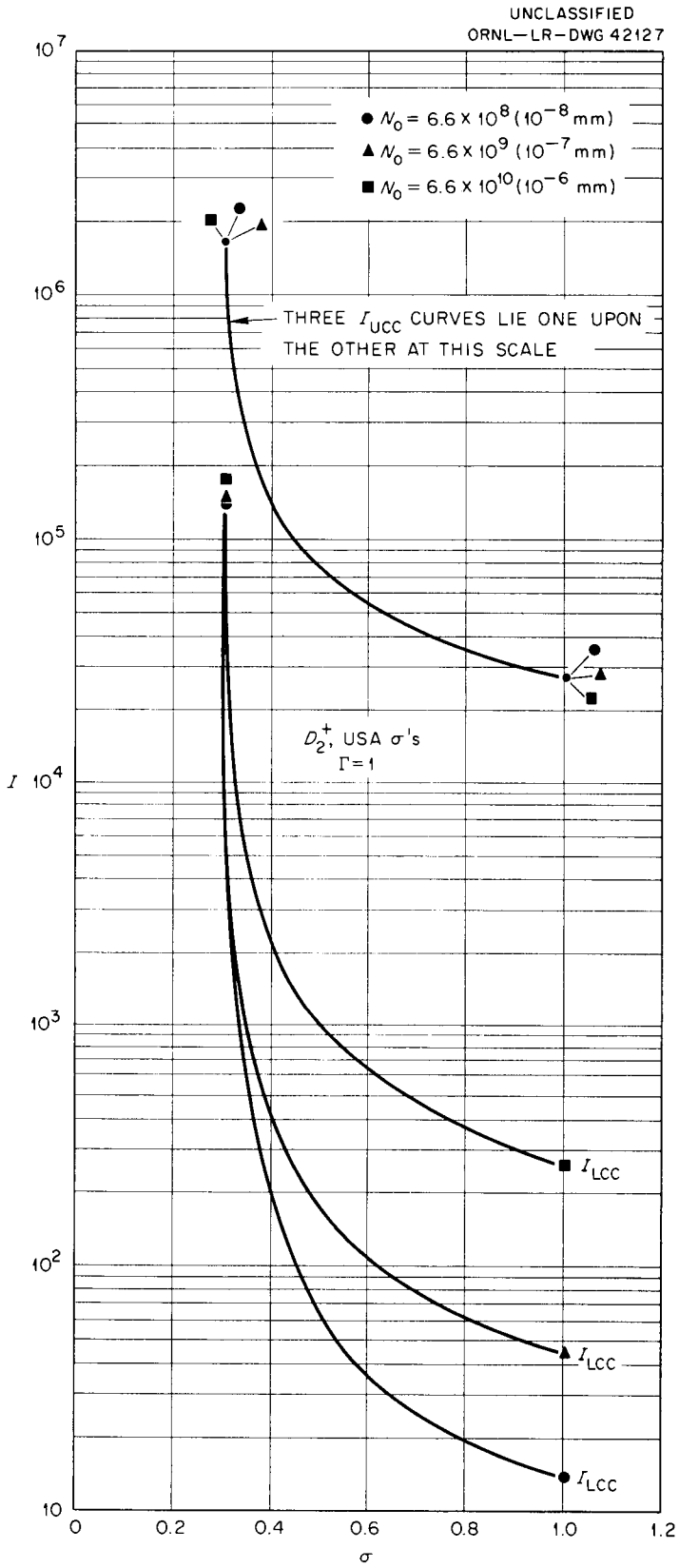
UNCLASSIFIED
ORNL—LR—DWG 42127
● $N_0 = 6.6 \times 10^8 (10^{-8}$ mm)
▲ $N_0 = 6.6 \times 10^9 (10^{-7}$ mm)
■ $N_0 = 6.6 \times 10^{10} (10^{-6}$ mm)
THREE I_{UCC} CURVES LIE ONE UPON THE OTHER AT THIS SCALE
D_2^+, USA σ's
$\Gamma = 1$
I_{LCC}
I_{LCC}
I_{LCC}
I
10^7
10^6
10^5
10^4
10^3
10^2
10
0
0.2
0.4
0.6
0.8
1.0
1.2
σ

Fig. 18.

UNCLASSIFIED
ORNL-LR-DWG 42128

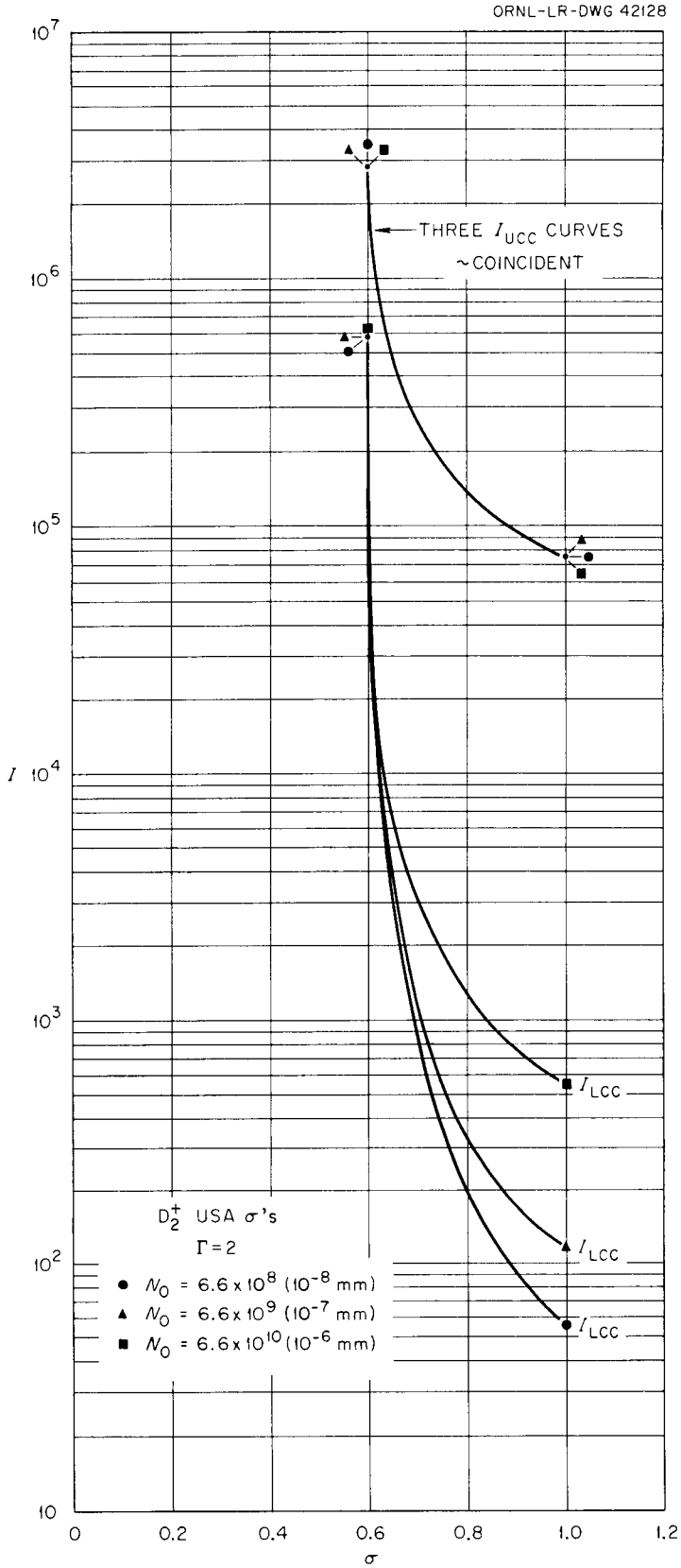

Fig. 19.

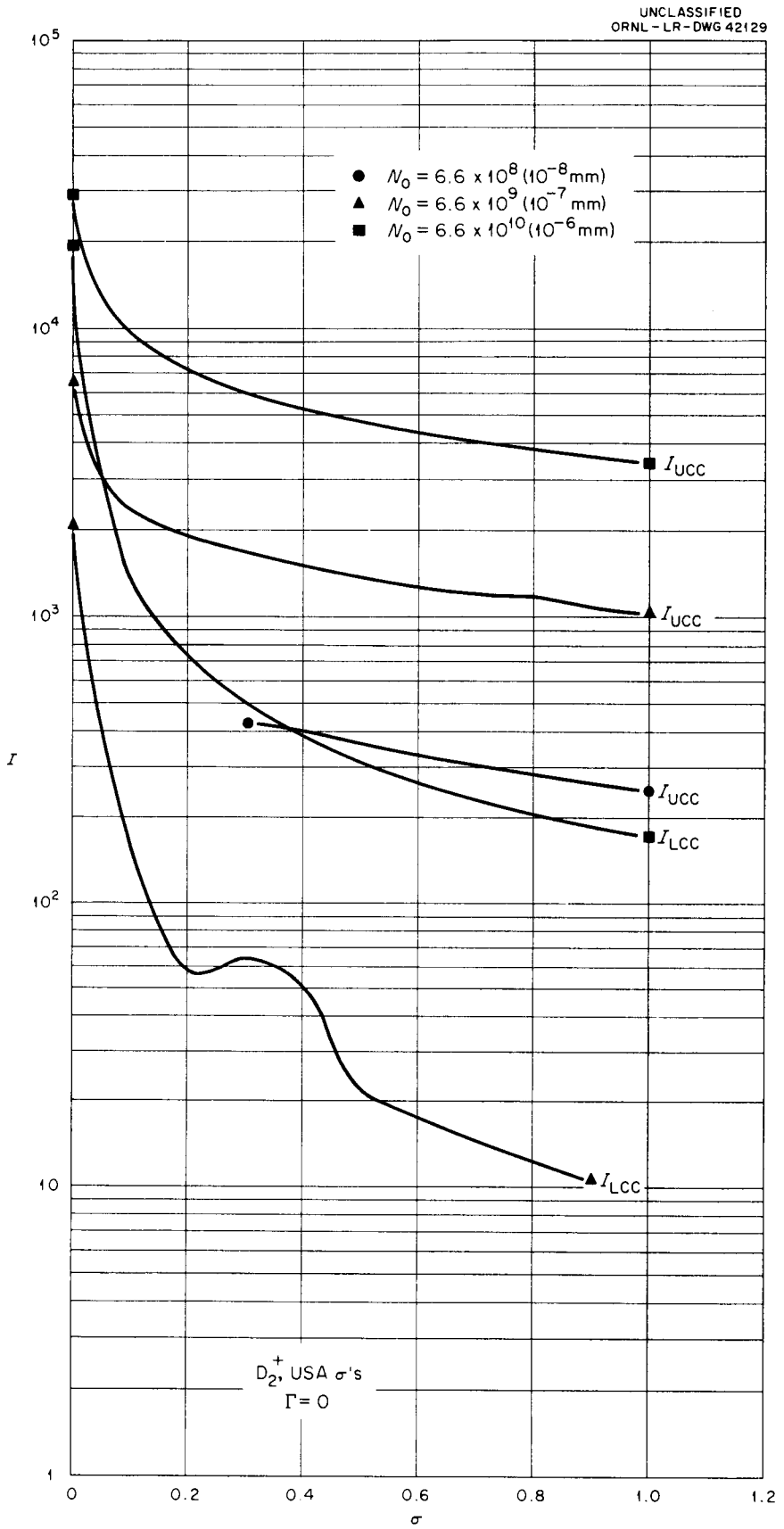
UNCLASSIFIED
ORNL - LR - DWG 42129
$N_0 = 6.6 \times 10^8 (10^{-8}$ mm)
$N_0 = 6.6 \times 10^9 (10^{-7}$ mm)
$N_0 = 6.6 \times 10^{10} (10^{-6}$ mm)
I_{UCC}
I_{UCC}
I_{UCC}
I_{LCC}
I_{LCC}
D_2^+, USA σ's
Γ = 0
10^5
10^4
10^3
10^2
10
1
I
0
0.2
0.4
0.6
0.8
1.0
1.2
σ

Fig. 20.

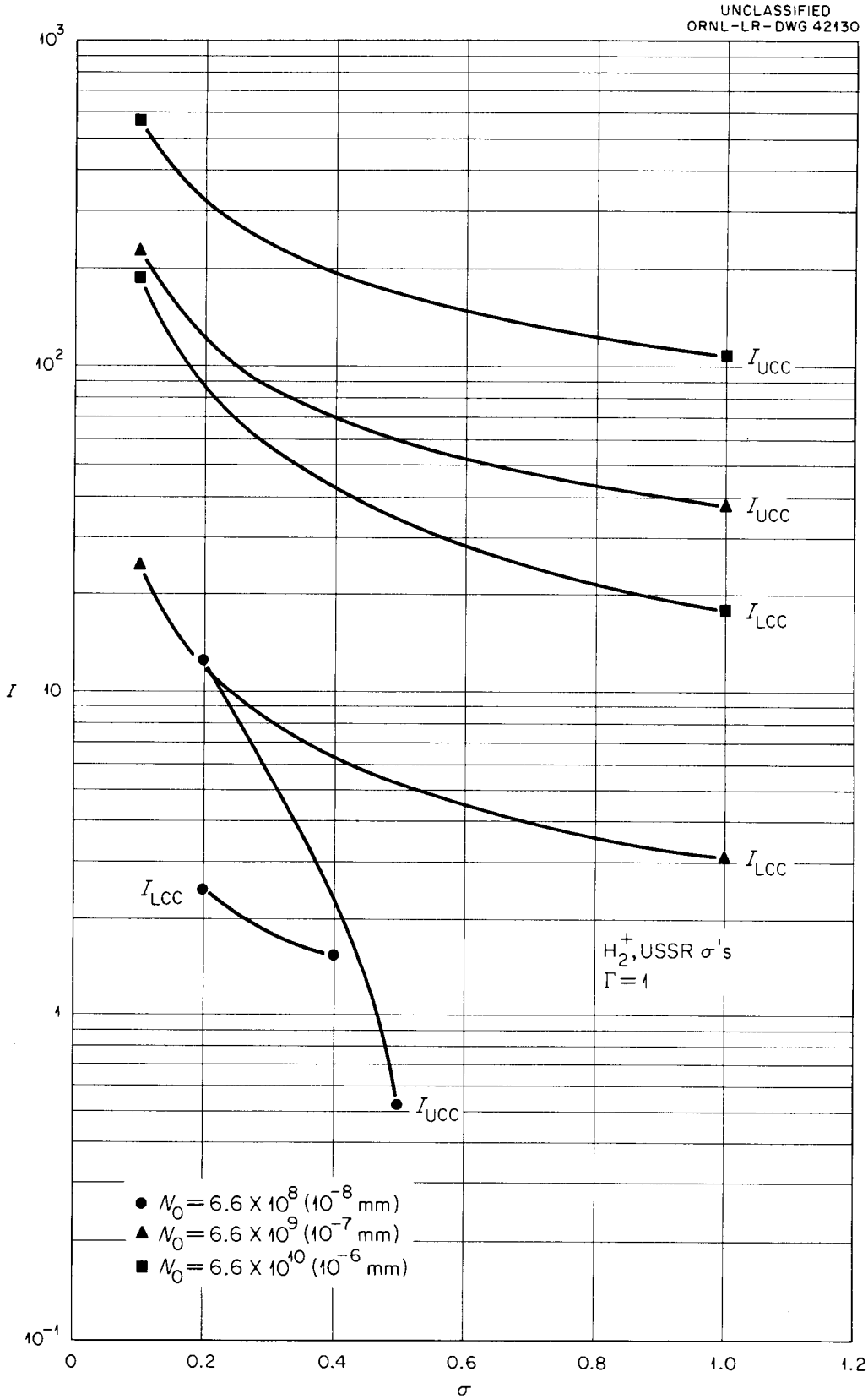
UNCLASSIFIED
ORNL-LR-DWG 42130
10^3
10^2
10
1
10^{-1}
I
I_{UCC}
I_{UCC}
I_{LCC}
I_{LCC}
I_{LCC}
I_{UCC}
H_2^+, USSR σ's
$\Gamma = 1$
● $N_0 = 6.6 \times 10^8$ (10^{-8} mm)
▲ $N_0 = 6.6 \times 10^9$ (10^{-7} mm)
■ $N_0 = 6.6 \times 10^{10}$ (10^{-6} mm)
0
0.2
0.4
0.6
0.8
1.0
1.2
σ

Fig. 21.

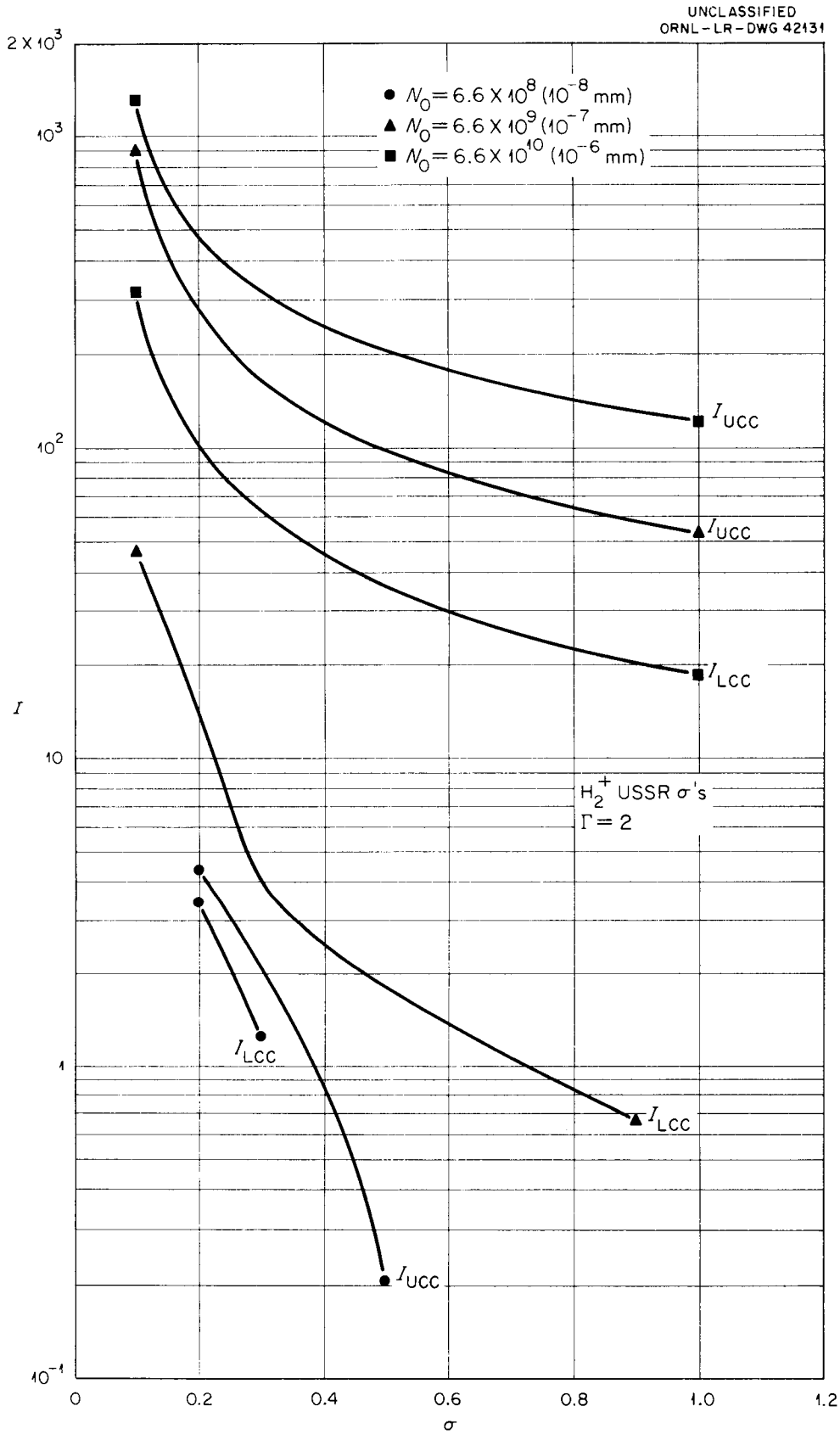
UNCLASSIFIED
ORNL-LR-DWG 42131
● $N_0 = 6.6 \times 10^8$ (10^{-8} mm)
▲ $N_0 = 6.6 \times 10^9$ (10^{-7} mm)
■ $N_0 = 6.6 \times 10^{10}$ (10^{-6} mm)
I_{UCC}
I_{UCC}
I_{LCC}
I_{LCC}
I_{LCC}
I_{UCC}
H_2^+ USSR σ's
$\Gamma = 2$
I
σ
2×10^3
10^3
10^2
10
1
10^{-1}
0
0.2
0.4
0.6
0.8
1.0
1.2

Fig. 22.

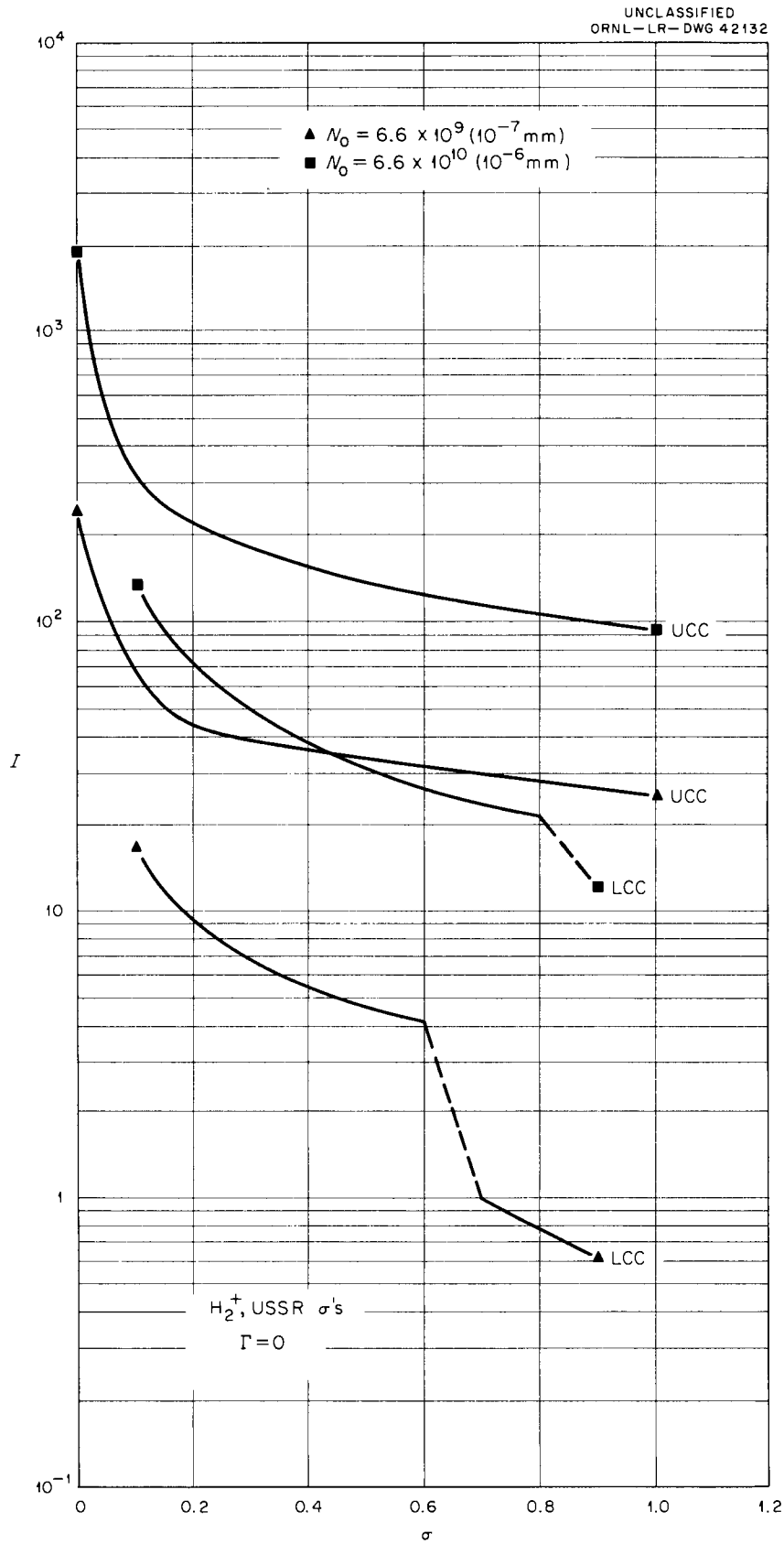
UNCLASSIFIED
ORNL-LR-DWG 42132
▲ $N_0 = 6.6 \times 10^9 (10^{-7} mm)$
■ $N_0 = 6.6 \times 10^{10} (10^{-6} mm)$
UCC
UCC
LCC
LCC
H_2^+, USSR σ's
Γ = 0
I
σ
10^4
10^3
10^2
10
1
10^{-1}
0
0.2
0.4
0.6
0.8
1.0
1.2

Fig. 23.

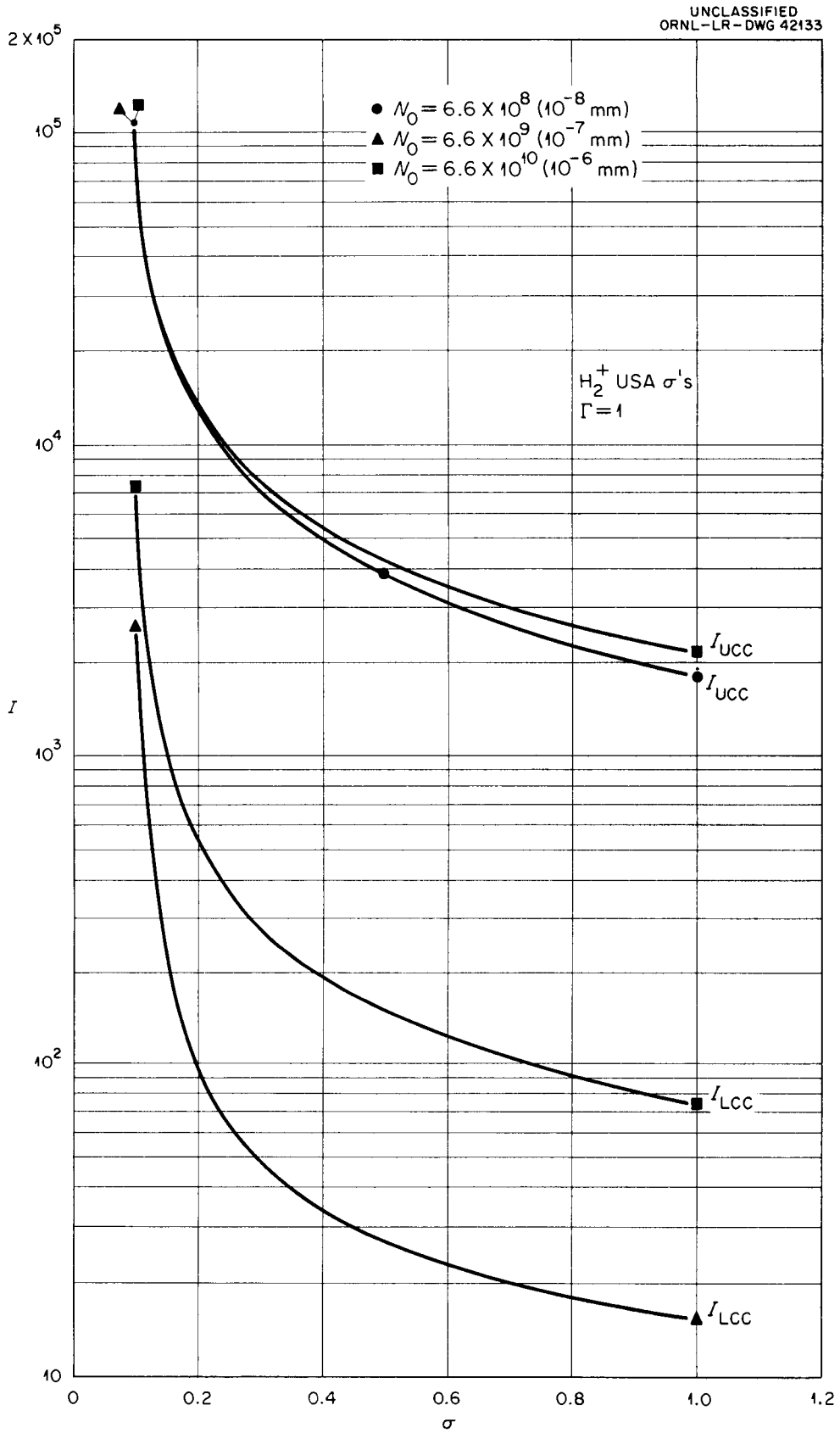
UNCLASSIFIED
ORNL-LR-DWG 42133
2 X 10^5
10^5
10^4
10^3
10^2
10
I
0
0.2
0.4
0.6
0.8
1.0
1.2
σ
● N0 = 6.6 X 10^8 (10^-8 mm)
▲ N0 = 6.6 X 10^9 (10^-7 mm)
■ N0 = 6.6 X 10^10 (10^-6 mm)
H2+ USA σ's
Γ = 1
IUCC
IUCC
ILCC
ILCC

Fig. 24.

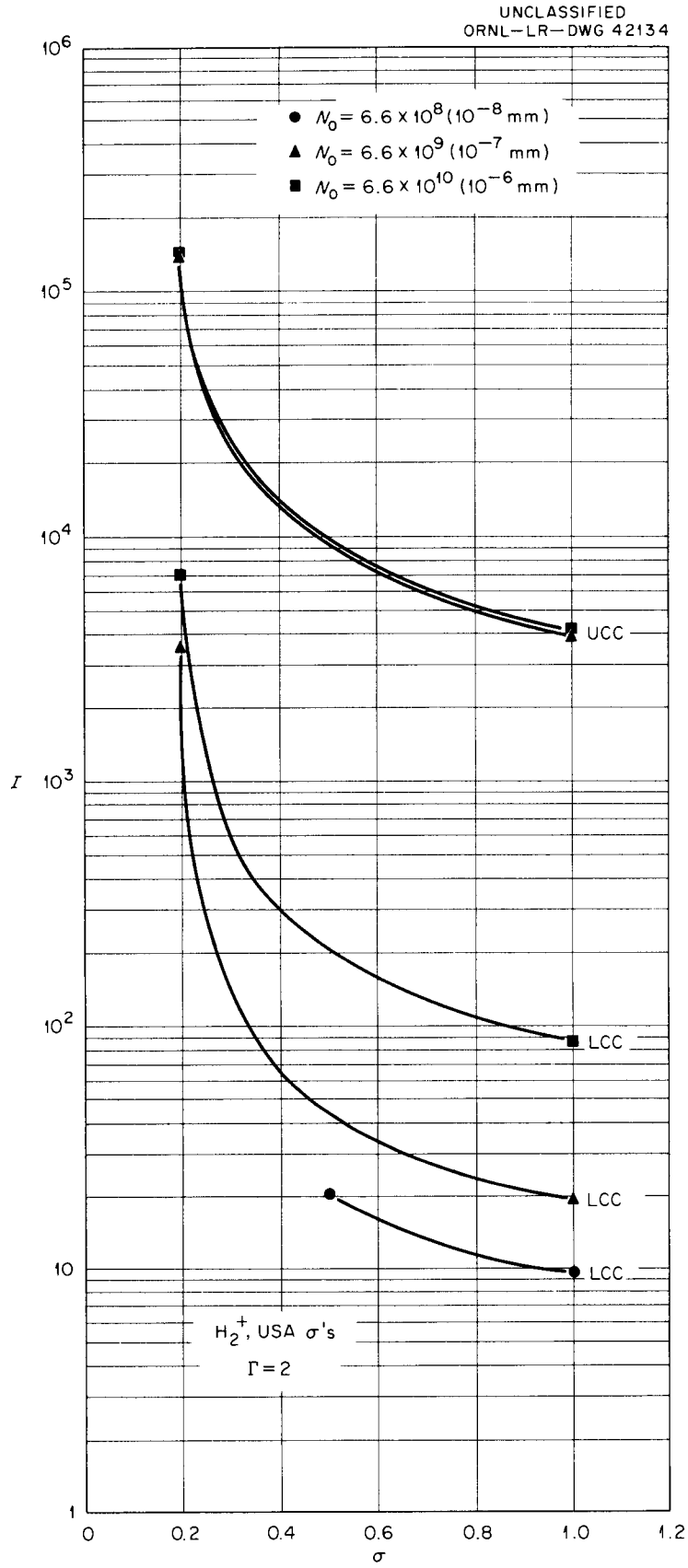
UNCLASSIFIED
ORNL-LR-DWG 42134
$N_0 = 6.6 \times 10^8 (10^{-8}$ mm)
$N_0 = 6.6 \times 10^9 (10^{-7}$ mm)
$N_0 = 6.6 \times 10^{10} (10^{-6}$ mm)
UCC
LCC
LCC
LCC
H_2^+, USA σ's
Γ = 2
I
10^6
10^5
10^4
10^3
10^2
10
1
0
0.2
0.4
0.6
0.8
1.0
1.2
σ

Fig. 25.

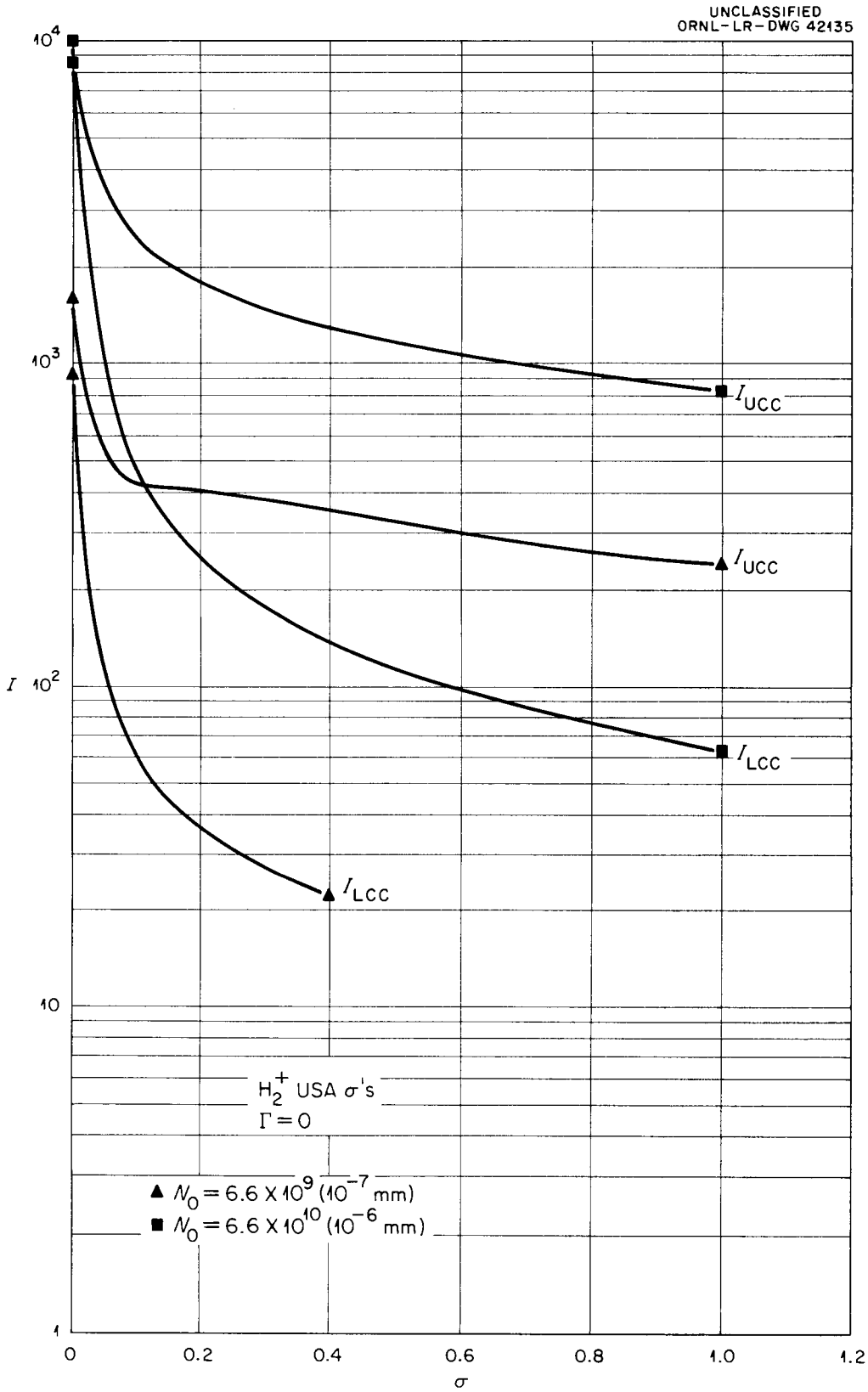
UNCLASSIFIED
ORNL-LR-DWG 42135
10^4
10^3
10^2
10
1
I
I_{UCC}
I_{UCC}
I_{LCC}
I_{LCC}
H_2^+ USA σ's
Γ = 0
▲ $N_0 = 6.6 \times 10^9$ (10^{-7} mm)
■ $N_0 = 6.6 \times 10^{10}$ (10^{-6} mm)
0
0.2
0.4
0.6
0.8
1.0
1.2
σ

Fig. 26.

I am greatly indebted to M. E. LaVerne for his patient and careful handling of the numerical calculations. I am also most indebted to R. C. Gilbert and R. E. Hester for calling my attention to the possibility of multiple roots in the gas breakup case.

APPENDIX A

THE PATH LENGTH L CONSIDERED AS A FIXED RANGE

It is not entirely clear whether the path length L should be considered to be a mean-free-path (as it is in the text) or a fixed range. If all injected particles entered at the same spatial point with the same angle then they would all ultimately strike some obstacle after traversing a fixed path length (in the absence of transient perturbations). More realistically, the injected beam has a rather wide spread in angle. The long path length and nonuniform magnetic field then produce a great deal of orbital precession and randomization and a statistical factor (i.e., a mean free path) would seem to be more correct. Actually the calculation below indicates that the difference is not important numerically, anyway.

Let us calculate the steady-state trapping rate if there is a fixed path length L. This is obviously

$$= 1 - e^{-(\hat{N}_o \sigma_B{}^o + n_+ \sigma_B{}^+)L} \tag{A1}$$

which should be compared with Eq. (4). If we define

$$x = (\hat{N}_o \sigma_B{}^o + n_+ \sigma_B{}^+)L \tag{A2}$$

then the ratio of these two expressions is:

$$R(x) = \frac{(1 - e^{-x})(1 + x)}{x} \tag{A3}$$

This ratio approaches unity for x very small and for x very large compared to unity. The table below lists numerical values of R for several values of y, where $y = e^{-x}$.

$y(\equiv e^{-x})$	0	.1	.2	.3	.4	.5	.6	.7	.8	.9	1.0
R	1	1.29	1.30	1.28	1.25	1.22	1.18	1.14	1.10	1.05	1

APPENDIX B

EXTENSION OF THE DCX BURNOUT FORMULA TO INCLUDE ION-PUMPING

An approximate expression for the critical current has been derived in reference 1 and 2. We shall now derive it in a different way and then generalize to include ion-pumping. Let us define "burnout" to be that point at which the mean-free-path of a neutral entering the plasma becomes equal to the mean chord length of the plasma volume. In the notation of this report:

$$\lambda = \bar{\ell} \tag{B1}$$

or

$$\frac{v_o}{v n_+ \sigma_d^+} = \bar{\ell} \tag{B2}$$

Now, since mirror loss is negligible at this point, the density is directly related to the input current by the lifetime against charge exchange. Thus

$$n_+ V = I \tau_{cx} \tag{B3}$$

$$= \frac{I}{\bar{n}_o \sigma_{cx} v} \tag{B4}$$

Upon substitution of Eq. (B4) in Eq. (B2), we have

$$I_{crit} = \bar{n}_o \frac{\sigma_{cx}}{\sigma_d^+} \frac{v_o V}{\bar{\ell}} \tag{B5}$$

Now

$$\bar{\ell} = \frac{4V}{S} \tag{B6}$$

and, by reference 2, Eqs. (2) and (7),

$$\bar{n}_o = \frac{\hat{N}_o}{1 + \frac{\bar{\ell}}{\lambda}} \tag{B7}$$

$$= \frac{\hat{N}_o}{2} \text{ at burnout.} \tag{B8}$$

where $\hat{N}_o$ is the neutral density external to the plasma. Hence

$$I_{crit} = \frac{\hat{N}_o}{2} \frac{v_o S}{4} \frac{\sigma_{cx}}{\sigma_d^+} \tag{B9}$$

This differs by a factor of 2 from the result given in reference 1. Of course, one cannot say which one is more "correct." Burnout is not a precisely defined event and either approximate expression is a useful measure of its region of onset.

The external density, $\hat{N}_o$, is determined by the balance of wall outgassing, ion pumping, external pumping, and backstreaming from the injected beam precisely as in Section I of the text. Hence, by Eq. (13), we have

$$\hat{N}_o = \frac{\frac{\Gamma}{\theta} I + N_o}{1 + \frac{\sigma}{\Theta} \frac{n_+ \sigma_d^+ vV}{1 + \frac{\bar{\ell}}{\lambda}}} \tag{B10}$$

At burnout, Eqs. (B1) and (B2) apply, which gives

$$\hat{N}_o = \frac{\frac{\Gamma}{\theta} I + N_o}{1 + \frac{\sigma V v_o}{2\theta \bar{\ell}}} \tag{B11}$$

Upon substitution of Eq. (B11) in Eq. (B9) and rearranging, we find

$$I_{crit} = \frac{N_o \frac{v_o S}{8} \frac{\sigma_{cx}}{\sigma_d^+}}{1 + \frac{S v_o}{8\theta}\left(\sigma - \Gamma \frac{\sigma_{cx}}{\sigma_d^+}\right)} \tag{B12}$$

It should be noted that burnout will be possible only if

$$\frac{\sigma_{cx}}{\sigma_d^+} \Gamma < \sigma + 2 \frac{\theta \bar{\ell}}{V v_o} \tag{B13}$$

which differs from Eq. (32) only by a factor of 2 in the last term. Again this difference arises from the slightly different approximations we have used.

INTERNAL DISTRIBUTION

1. C. E. Center
2. Biology Library
3. Health Physics Library
4-5. Central Research Library
6. Reactor Experimental Engineering Library
7-26. Laboratory Records Department
27. Laboratory Records, ORNL R.C.
28. A. M. Weinberg
29. L. B. Emlet (K-25)
30. J. P. Murray (Y-12)
31. J. A. Swartout
32. E. H. Taylor
33. E. D. Shipley
34. A. H. Snell
35. E. P. Blizard
36. M. L. Nelson
37. W. H. Jordan
38. R. A. Charpie
39. S. C. Lind
40. F. L. Culler
41. A. Hollaender
42. J. H. Frye, Jr.
43. M. T. Kelley
44. J. L. Fowler
45. R. S. Livingston
46. K. Z. Morgan
47. T. A. Lincoln
48. A. S. Householder
49. C. P. Keim
50. C. S. Harrill
51. C. E. Winters
52. D. S. Billington
53. R. H. Ritchie
54. D. Phillips
55. A. J. Miller
56. M. J. Skinner
57. R. R. Dickison
58. J. A. Harvey
59. H. E. Seagren
60. F. C. Maienschein
61. L. B. Holland
62. A. D. Callihan
63. R. R. Coveyou
64. W. Zobel
65. F. L. Keller
66. C. D. Zerby
67. D. K. Trubey
68. S. K. Penny
69. R. W. Peelle
70. F. S. Alsmiller
71. R. G. Alsmiller, Jr.
72. C. F. Barnett
73. P. R. Bell
74. E. S. Bettis
75. R. E. Clausing
76. R. A. Dandl
77. L. Dresner
78. T. K. Fowler
79. W. F. Gauster
80. G. G. Kelley
81. R. J. Kerr
82. N. H. Lazar
83. J. S. Luce
84. R. J. Mackin, Jr.
85. J. R. McNally, Jr.
86. C. D. Moak
87. R. V. Neidigh
88. J. H. Neiler
89. C. E. Normand
90. M. Rankin
91. C. H. Weaver
92. T. A. Welton
93. A. Zuker
94. E. G. Harris
95-99. A. Simon
100. P. M. Reyling
101. F. L. Friedman (consultant)
102. H. Goldstein (consultant)
103. H. Hurwitz, Jr. (consultant)
104. L. W. Nordheim (consultant)
105. R. F. Taschek (consultant)
106. ORNL-Y-12 Technical Library, Document Reference Section

EXTERNAL DISTRIBUTION

107. Division of Research and Development, AEC, ORO
108-701. Given distribution as shown in TID-4500 (15th ed.) under Controlled Thermonuclear Processes Category (75 copies - OTS)